Renewable and Sustainable Energy Reviews 56 (2016) 1351–1371

Contents lists available at ScienceDirect

Renewable and Sustainable Energy Reviews

journal homepage: www.elsevier.com/locate/rser

A review on small scale wind turbines

Abhishiktha Tummala [a], Ratna Kishore Velamati [a,*], Dipankur Kumar Sinha [b], V. Indraja [c], V. Hari Krishna [d]

[a] Department of Mechanical Engineering, Amrita School of Engineering, Ettimadai Campus, Amrita Vishwa Vidyapeetham, Coimbatore, 641112, India
[b] Sanmar Industries, Tirchy, India
[c] Department of Industrial and Systems Engineering, North Carolina State University, Raleigh, USA
[d] Cognizant Technology Solutions, India

ARTICLE INFO

Article history:
Received 12 May 2014
Received in revised form
16 September 2015
Accepted 10 December 2015
Available online 30 December 2015

Keywords:
Small scale wind turbines
Aero acoustics
Aerofoil
Rotor diameter

ABSTRACT

Meeting future world energy needs while addressing climatic changes has led to greater strain on conventional power sources. One of the viable sustainable energy sources is wind. But the installation large scale wind farms has a potential impact on the climatic conditions, hence a decentralized small scale wind turbines is a sustainable option. This paper presents review of on different types of small scale wind turbines i.e., horizontal axis and vertical axis wind turbines. The performance, blade design, control and manufacturing of horizontal axis wind turbines were reviewed. Vertical axis wind turbines were categorized based on experimental and numerical studies. Also, the positioning of wind turbines and aero-acoustic aspects were presented. Additionally, lessons learnt from various studies/countries on actual installation of small wind turbines were presented.

Contents

1. Introduction

Gross Domestic Product (GDP) is the major factor to judge the development of a country [1]. GDP represents the economic

* Corresponding author. Tel.: +918122857821.
E-mail addresses: ratnakishore@cb.amrita.edu, ratnavk@gmail.com (R.K. Velamati).

http://dx.doi.org/10.1016/j.rser.2015.12.027
1364-0321/

growth of a country which is closely related to the amount of the power produced by the nation. To have a sustainable economic growth, a nation should have the resources to continuously produce energy. But due to the precipitous depletion of the conventional energy sources and the increase in the CO_2 emissions, the demand for a sustainable and a reliable alternate source of energy has been increasing day by day. Wind energy and solar energy are two sources of energy that hold a chance to serve the purpose. Wind energy, being renewable provides a great opportunity to generate energy due to its abundance.

Wind turbines are those which convert the kinetic energy present in the wind to mechanical energy and eventually into electricity. The history of wind turbines originates around 200 B.C somewhere in Persia but the first practical wind mills were developed in 7th century in Iran and were called the Sistan wind mills. Wind mills were effectively used in farms for producing electricity and pumping water in 1930's in USA. The first utility grid-connected wind turbine was built by John Brown & Co in 1951. The total capacity of wind power by the end of 2014 was around 369.6 GW and is expected to touch 666.1 MW by the end of 2019 [2].

Various countries, in order to meet their growing power demand are installing large scale wind farms both on shore and off shore. In 2014, China has installed capacity of around 114,609 MW of wind energy contributing 31.0% of the total wind power followed by USA, Germany, Spain and India which produce 65,879 MW, 39,165 MW, 22,987 MW and 22,465 respectively as shown in Fig. 1 [3]. In the current scenario large scale wind turbines farms (like offshore wind farm "London Array" which is around 100 km^2 and onshore wind farm "Alta Wind Energy Centre" which is around 36.5 km^2) are required in order to match the increasing power demand. This will lead to expansion of the wind farms and finally would result in large scale continental wind farms.

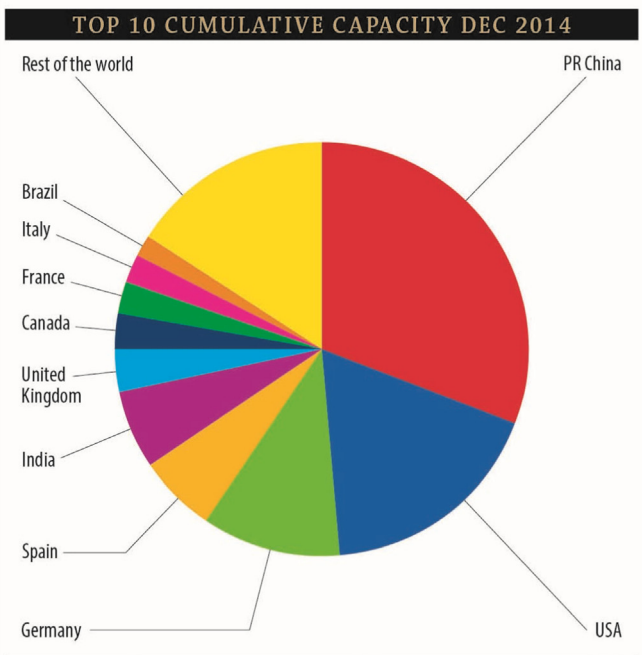

Country	MW	% SHARE
PR China	114,609	31.0
USA	65,879	17.8
Germany	39,165	10.6
Spain	22,987	6.2
India	22,465	6.1
United Kingdom	12,440	3.4
Canada	9,694	2.6
France	9,285	2.5
Italy	8,663	2.3
Brazil*	5,939	1.6
Rest of the world	58,473	15.8
Total TOP 10	**311,124**	**84.2**
World Total	**369,597**	**100**

** Projects fully commissioned, grid connection pending in some cases* *Source: GWEC*

Fig. 1. Highest cumulative installed capacity in 2014 [3].

The effect of large scale wind farms on the climatic conditions has been studied by various authors. Wang et al. [4] have performed simulations using a three dimensional climatic model in order to study the various potential climatic effects of future large scale wind farm installation over land and ocean. The simulations were run on a global scale for a period of 60 years as the temperature changes need a longer duration to show the gradual impact. It was observed that the installation of wind turbines in order to meet 10–15% of global energy demand might cause surface warming by increasing the temperature by 1 °C on land. Similar simulations for the 1 °C increase in temperature over the oceans have also been computed by increasing the ocean surface drag but a further study has to be done on its validation. Fig. 2 shows the temperature changes in one of the models due to the deployment of large scale wind turbines over the land in order to generate 158 EJ/year. All the above conclusions can only be made after considering the special or new parameters that affect the wind turbines. Due to nonlinear variation of climatic changes with surface roughness, defining the optimal arrangement of wind turbines is challenging. Climatic effects increase with the power generated and decrease with conversion efficiency, leaving out the potential environmental effects on birds, weather radar, ambient noise levels etc.

Fiedler et al. [5] have performed simulations for 62 warm seasons on a regional climatic model, and observed that there was 1% increase the precipitation rate. It was also seen that a larger rate of precipitation has occurred for a larger wind farm [6,7]. From the above results a conclusion can be drawn that installing large scale wind farms might lead to significant weather changes, so there arises a need to effectively use this wind energy without causing any adverse effects to the atmosphere.

The large scale wind farms are not a sustainable viable option for renewable power production. The best option available is by installing the decentralized grid system i.e., by using small scale wind turbines. Small scale wind turbines produce power around 10 kW which is sufficient for our domestic needs. This energy can be effectively utilized so that the energy extracted from the conventional resources could be saved for a larger period of time. Hence there arises the need to understand the characteristics of small scale wind turbines. The majority of work on small scale wind turbines was done over the past few years. The disadvantages of small wind turbines are high initial cost, effective placement, wind fluctuation, change in wind direction and also aero-acoustic noise.

This paper presents a detailed literature review on small scale wind turbines. Initially, scaling of wind turbines was illustrated in order to identify small scale wind turbines. Then, the general classification of the wind turbines was explained. After that, various aspects of horizontal axis wind turbine (HAWT's) like performance, blade design, control and manufacturing were reviewed. Next, review of various kinds of Vertical axis wind turbines (VAWT) was presented. Darrieus type VAWT was reviewed in two sections, experimental and numerical analysis. Also, positioning of wind turbines and aeroacoustics of small scale wind turbines were presented.

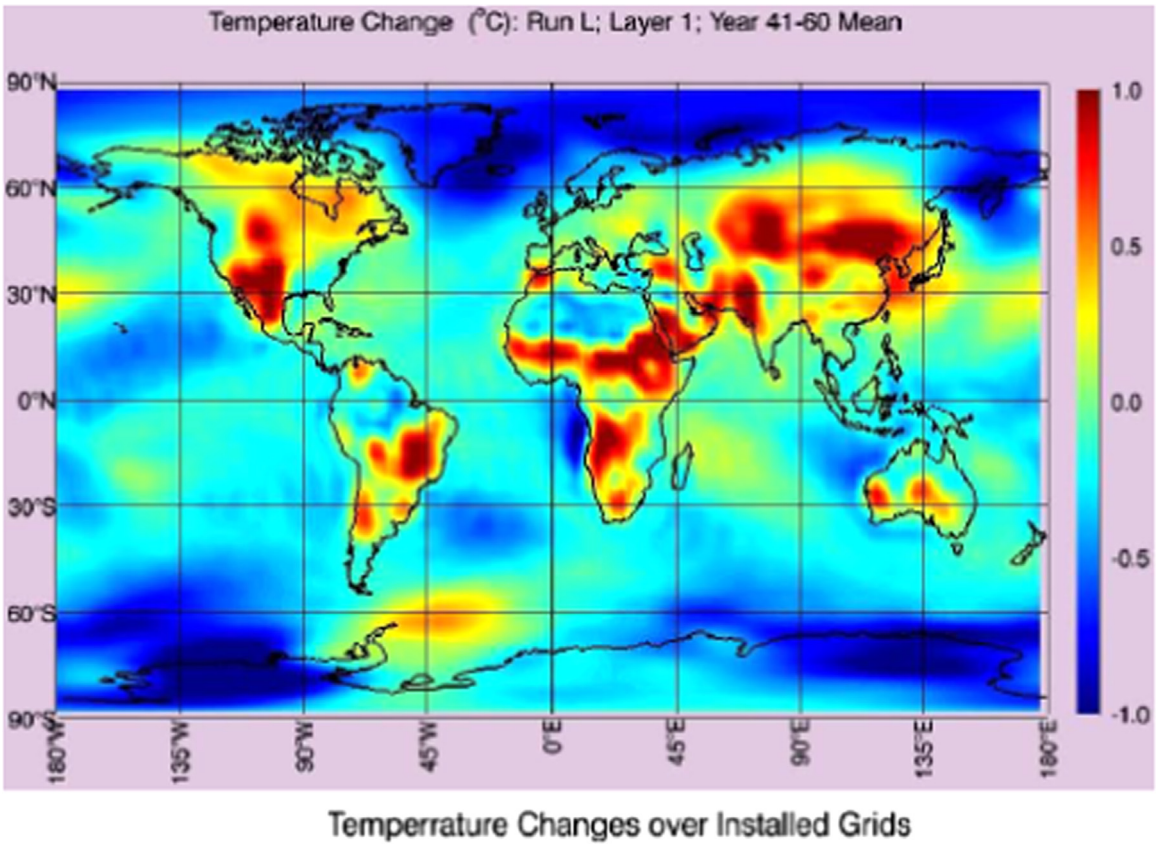

Fig. 2. Temperature changes due to the deployment of large scale wind turbines [4].

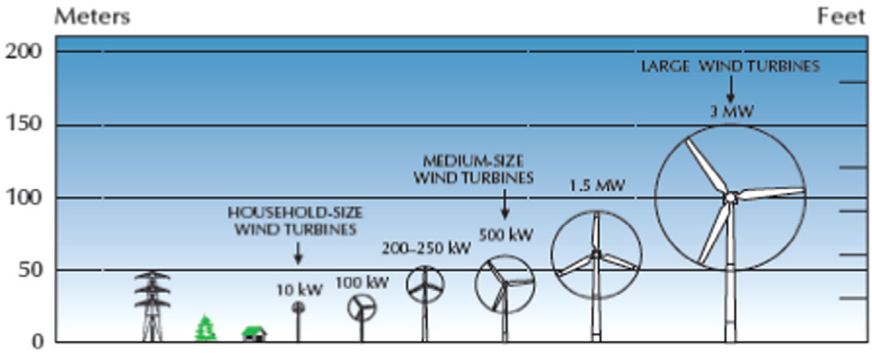

Fig. 3. Classification of wind turbines based on rotor diameter.

2. What is a small scale wind turbine?

Fig. 3 shows the classification of wind turbines based on rotor diameter. A typical large scale wind turbine is one which has a rotor diameter ranging from 50 m to 100 m. It produces power between 1 and 3 MW. When compared to large scale wind turbines, small scale wind turbines are those which have their rotor diameter ranging from 3 m to 10 m and having a power capacity of 1.4–20 kW. Table 1 demonstrates the classification of wind turbines based on power rating. Small scale wind turbines which have a nominal power rating of 50 W produce more costly electricity than the medium and large scale wind turbines especially in poor wind sites. They are also handy in some autonomous applications which require a very high level of reliability. These wind turbines can be used as a reliable source of energy when they are sized properly and are used at their optimum conditions. They can also become the source for producing socio-economically valuable energy for most of the developing countries. In locations which are far away from the grid power, these small scale turbines can act as a useful power source even in the developed countries. But the future of the continuous growth of small scale wind turbines

Table 1
Classification of HAWT based on rotor diameter and power rating.

		Rotor diameter (m)		Swept area (m^2)		Standard power rating (kW)	
Small scale	Micro	0.5	1.25	0.2	1.2	0.004	0.25
	Mini	1.25	3	1.2	7.1	0.25	1.4
	Household	3	10	7	79	1.4	16
Small commercial		10	20	79	314	25	100
Medium commercial		20	50	314	1963	100	1000
Large commercial		50	100	1963	7854	1000	3000

depends upon the cost at which it is being generated. Two major factors are the initial cost per W power and the unit cost per kW-h it produces. Given that these two factors are at an affordable rate, small scale wind turbines can become a potential source for power production. Hence the small scale wind turbines must be cost efficient. Hence it is very much necessary to study and understand the different kinds of small scale wind turbines available at present. Hence this paper presents a detailed review on small scale wind turbines.

3. Classification of small scale wind turbines

Small scale wind turbines can be classified based on two categories:

1. Classification based on axis of rotation:

   a. *Vertical Axis Wind Turbines:* Vertical axis wind turbines are those whose rotor axis is in vertical direction. These turbines do not have any yawing mechanism or self-starting capability. The generator location for these turbines is on ground and their height of operation is very low hence making them easier for maintenance. The ideal efficiency for these turbines is more than 70%.

The vertical axis wind turbines are classified into two major types:

(i) *Darrieus Wind Turbine:* The Darrieus wind turbine is a type of vertical axis wind turbine which consists of a number of straight or curved blades mounted on a vertical framework. These turbines work from the lift forces produced during rotation.
(ii) *Savonius Wind Turbine:* Savonius wind turbines are drag based wind turbines consisting of two to three scoops. These turbines have an 'S' shaped cross section when looked from above. As they move along the wind, they experience lesser drag and this difference in drag helps these turbines to spin. Due to the drag, the efficiency of these turbines is less when compared to other types of turbines.

   b. *Horizontal Axis Wind Turbines:* Turbines whose rotor axis is in the horizontal direction are called as Horizontal Axis Wind Turbines. Unlike vertical axis wind turbines, horizontal axis wind turbines have the ability to self-start and yaw. These turbines are highly dependent on wind direction and hence they are generally operated at higher heights than the VAWT. The ideal efficiency for these turbines is between 50% and 60%.

2. Classification based on lift and drag forces

   a. *Lift type:* Horizontal axis wind turbines and Darrieus wind turbine (vertical axis wind turbine).
   b. *Drag type:* Savonius wind turbine.

4. Horizontal axis wind turbines

As mentioned in Section 3, horizontal axis wind turbines are turbines in which the rotor axis is in the horizontal direction. Since large scale wind farms (generally HAWT) have potential impact on the climatic conditions, work is being done in order to understand the performance characteristics of small scale HAWT by varying various parameters. The work done on small scale HAWT for various parameters has been presented in the upcoming sections.

4.1. Performance of small scale HAWT

This section presents the work done by various authors on the performance characteristics of small scale HAWT.

Freere et al. [8] have performed a case study on a low cost wind turbine MG4520 as shown in Fig. 4. A 3-bladed turbine of rotor diameter 2.1 m was tested in a wind tunnel up to a wind speed of 13 m/s. The blade characteristics were calculated as a function of wind speed, yaw angle, with and without a nose cone. At various wind speeds, the values of tip speed ratio (TSR) varied from 2 to 8 and the maximum C_p of 0.2 occurred at a TSR 6. No considerable change in the blade power output was observed with the presence of nose cone. It was also observed that at a particular wind speed, the maximum power value decreased with the increase in yaw angle. Overall study suggests that large improvements in the performance of the blades are possible and would need controller and generator to be altered to avoid wind turbine stalling.

Refan et al. [9] verified experimentally and theoretically, the aerodynamic performance of an upwind, three-bladed, small HAWT as shown in Fig. 5. The applicability of the blade element momentum (BEM) theory for modeling the rotor performance for the case of small HAWTs with a small rotor of 2.2 m diameter was assessed in a wind tunnel up to a wind speed of 11 m/s. Using the BEM analysis, Wortmann FX 63 137 airfoil was selected for the tip

Fig. 4. MG4520 wind turbine [8].

Fig. 5. Wortmann FX 63 137 airfoil wind turbine [9].

region of the blade ($r > 0.59$ m) and NACA 6515 for the root region. The wind turbine has been tested in order to determine the power curve for a wide range of wind speeds. From the experimental data, the aerodynamic performance curve shows that for low speed tests, a maximum power of 470 W is obtained at 9 m/s and a high cut-in speed of the rotor at about 5 m/s. The results showed that over all predictions of the BEM theory were with-in the acceptance range as shown in Fig. 6. But the BEM theory prediction is more accurate for large scale wind turbines than small scale due to Reynolds number and three dimensionality effects. The main three-dimensional effects on the turbine rotor can be due to separation delay at the inboard sections radial flow and downwash effect, and tip vortex.

Performance testing of a small wind turbine rotor for low wind speed applications was done by Singh et al. [10]. A 2 bladed rotor was designed for low Re application and was fit to an Air-x marine 400 W wind turbine. The wind turbine rotor was of 1.26 m diameter. The rotor incorporated an exponential twist and taper distribution and the AF300 airfoil for increased aerodynamic performance at low wind speeds. At different pitch angles of 15°, 18°, and 20°, the performance was studied. Performance of Air-X with the 2-bladed rotor was compared to the baseline 3 bladed rotor (rotor diameter 1.16 m). It was observed that the rotor achieved C_p (coefficient of power) values of 0.l, 0.217 and 0.255 at the wind speeds of 4, 5 and 6 m/s respectively while the baseline 3-bladed rotor achieved 0.052, 0.112 and 0.15 at these wind speeds as shown in Fig. 7. This shows that the 2 bladed rotors have better C_p in the low wind speed range of 3–7 m/s. At the optimum pitch, $\beta = 18°$, the 2-bladed rotor produced more than double the power than the baseline rotor. Only at the pitch angle of 15° and at a wind speed of 4 m/s, the power output of the baseline rotor coincided with that of the 2-bladed rotor.

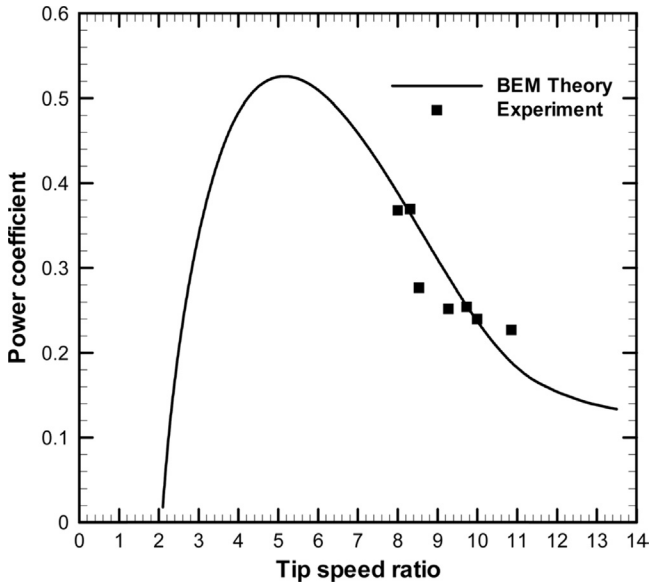

Fig. 6. Comparison of experimental and theoretical power coefficients [9].

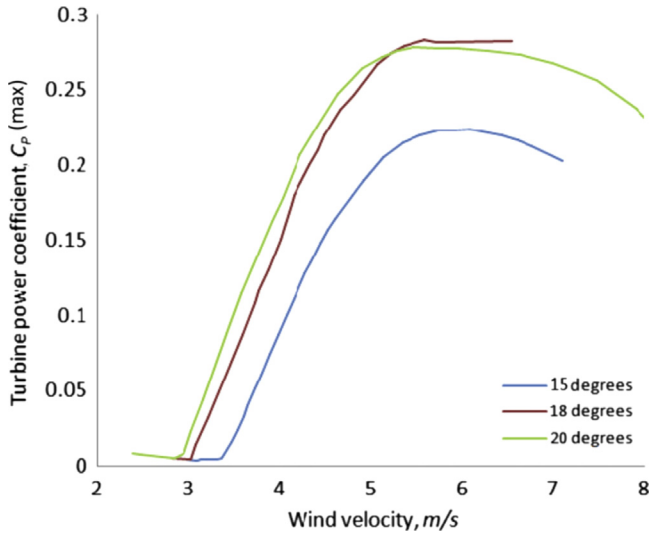

Fig. 7. Minimum power coefficient of the turbine as a function of wind velocity at different pitch settings [10].

The design and characterization of small scale wind energy portable turbine (SWEPT), of 39.4 cm rotor diameter operating below the wind speed of 5 m/s was done by Kishore et al. [11]. The prototype is shown in Fig. 8 below. Wind tunnel experimentation was done in order to examine the aerodynamic performance. Maximum coefficient of performance of 14% was obtained at optimal tip speed of 2.9 m/s. It had low cut in wind speed of 2.7 m/s and which gave 0.83 W of electric power at the rated wind speed of 5 m/s. A diffuser was designed for the SWEPT using CFD simulations to enhance the overall power output of a wind turbine. It was observed that the diffuser-augmented SWEPT of length approximately the same as the turbine's diameter could produce 1.4–1.6 times higher power output than a SWEPT without diffuser.

Hirahara et al. [12] have built and reported the performance of a very small scale, 4 bladed wind turbine μF500 of a rotor diameter of 500 mm, having NACA 2404 airfoil profile. Various tests were carried out on parameters such as the energy output, turbine speed, power coefficient, torque of the turbine at various free stream velocities. Particle Image Velocimetry (PIV) was employed to study the flow around the wind turbine and the influence of the turbulence. The results showed that the turbine has a good efficiency in the wind range of 8–12 m/s with net efficiency and power coefficient as 0.25 and 0.36 respectively. It showed good performance at lower tip speed ratios. The maximum power coefficient was about 0.40 when the tip speed ratio was 2.7. The approaching flow velocity and the accelerated flow field passing the blade tip was obtained by the flow visualization and PIV measurement around the wind turbine. The flow in actual case

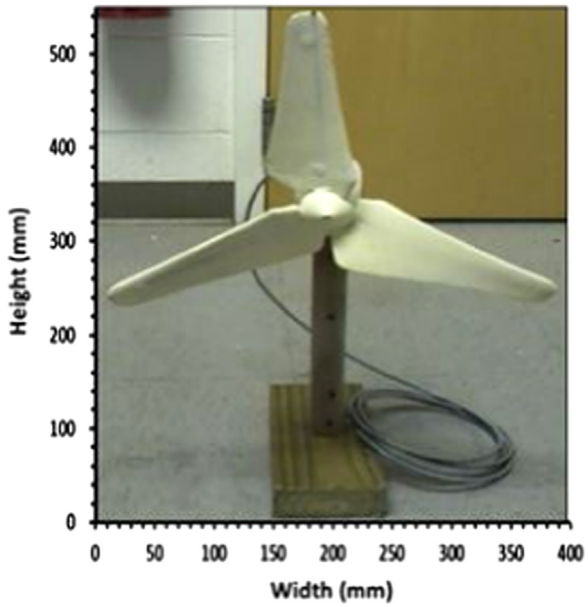

Fig. 8. First generation small-scale windmill prototype "SWEPT" [11].

and the ideal cases were compared and it was observed that flow in the actual case was 20% slower than the ideal case.

Duquette et al. [13] have conducted a numerical study in order to examine the impact of rotor solidity and blade number on the aerodynamic performance of small wind turbines. SG6043 airfoil was used for this study. Blade element momentum theory and lifting line based wake theory were utilized to assess the effects of blade number and solidity on rotor performance. An increase in power coefficients at lower tip speed ratios was observed with increase in the solidity. Also, the power coefficients increased with the increase in the blade number at a given solidity as shown in Fig. 9. An increase in the solidity from the conventional 5–7% to a range of 15–25% yielded higher maximum Cp values while lowering tip speed ratio at maximum Cp to 2–4. Lower tip speed ratios reduce structural requirements, blade erosion and noise levels. In addition, the high-torque characteristics of higher solidity rotors lower the cut-in speeds.

Matsumiya et al. [14] have conducted several field and track tests on a 1 kW small HAWT Airdolphin, which was designed to operate under wide range of wind speeds up to 50 m/s. These tests were conducted in two different regions- a) windy site, b) offshore site. A series of track tests demonstrated the stall operation concept under high winds as well as safety. Captureability ($CPT = P_{turbine}/P_{wind}$) and capacity factor ($CF = P_{turbine}/P_{rated}$) are the overall estimators with respect to the available wind power and the rated power by integrating over the entire range of wind speeds. As shown in Fig. 10, CPT and CF were plotted for various wind speeds. CF increases with annual mean wind speed for all values of k. On the other hand, CPT is significantly affected by the Weibull parameter k and annual mean wind speed as shown in Fig. 11. CPT reflects the underlying physics more as compared to CF and would not bring false indication like CF. Thus, CPT is a more suitable and fair parameter as a performance indicator. The power performance of Airdolphin was evaluated and we can expect total (or mean) capacity factor of 15%, 20%, and 25% at the sites of 6 m/s, 10 m/s, and 12 m/s of annual mean wind speed, respectively, for Weibull parameter $k=2$.

A study on small scale HAWT was carried out in order to investigate the effects of tunnel blockage on the power coefficient (in terms of blockage factor) in wind tunnel tests by Chen and Liou [15]. Under various test conditions, the blockage factor (BF) was determined by measuring the velocities at different points in the wind tunnel and the studies were carried out on a 6 bladed turbine having non-twisted, NACA 4415 profile blades and blade lengths of 30 cm, 24 cm and 14.5 cm. It was observed that the blockage effects increase as TSR and BR increase, and as β decreases. A plot of Cp vs. tips speed ration (TSR) was plotted at different pitch angles as shown in Fig. 12 indicating that the smaller the β value, the larger the C_{Pmax}. The C_{Pmax} occurs at larger TSR for smaller β. The tunnel blockage effect was small for small TSR, and BF approaches a constant value at a certain TSR, at which point the blades act like a solid wall. It was observed that the tunnel blockage effect and the decay rate of BF are larger for the 12-blade turbine than the 6-blade for the same TSR. It was also determined that no blockage correction is necessary for $\beta=25°$,

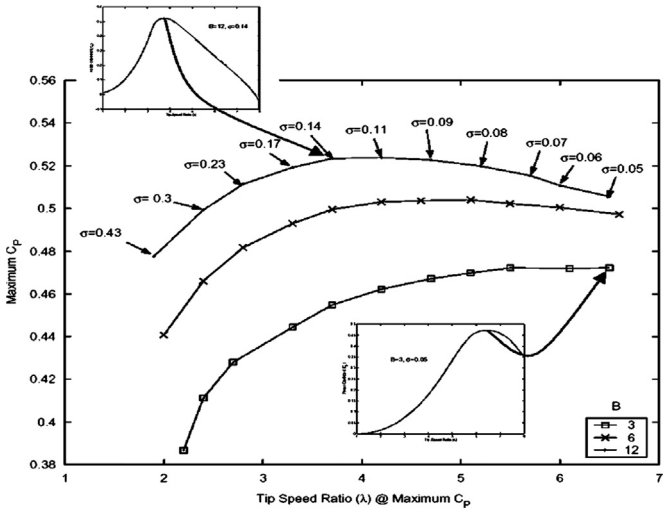

Fig. 9. Optimum design maximum C_P versus tip-speed ratio for various blade numbers (BEM analysis) [13].

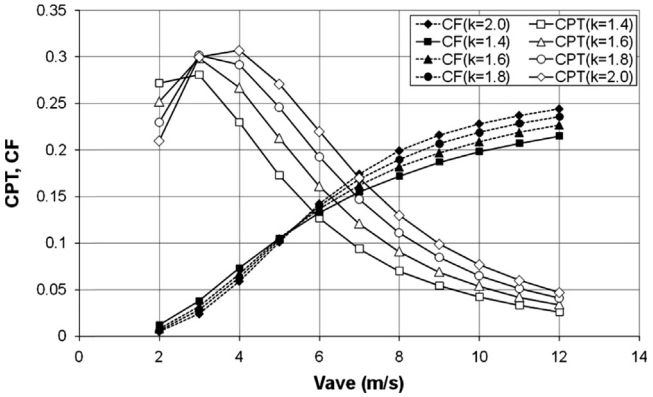

Fig. 11. Captureability and capacity factor of Airdolphin for different annual mean wind speeds and different Weibull parameters k [14].

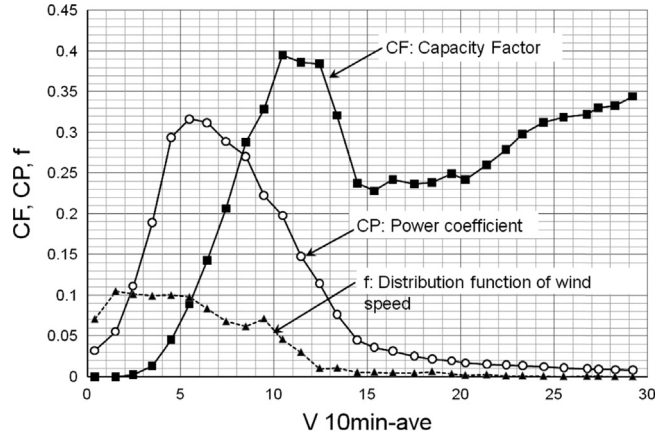

Fig. 10. Bin-averaged f, CF, and CP of Airdolphin no. 1 [14].

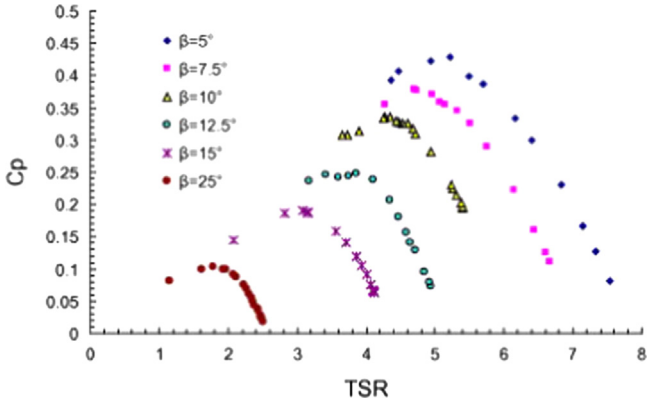

Fig. 12. Relationships between CP and TSR under six different β for 12 blades, $U\infty=8$ m/s and BR=28.3%. [15].

and the blockage correction is less than 5% for BR less than 10% and for TSR less than 1.5.

Habali et al. [16] have done the design of a blade and root for a blade length of 5 m. Procedure for selection of an airfoil section and the aerodynamic design of the blade for a small wind turbine are discussed in this work. Glass Fiber Reinforced Plastic, a composite material was used in designing the rotor blades. The airfoil FX66-S-196 is selected for the outboard region of the blade as it has a stable lift coefficient (C_L) at high angles of attack and the moment coefficient (C_m) is smooth and almost constant over the whole range of operating angles of attack. As the inboard region requires more material to withstand the higher stresses NACA 63-621 was chosen. The dimensions of the rotor were calculated based on the rated power (20 kW). The stress calculations at the root of the blade were done yielding the root dimensions. To carry out the stress analysis on the blade various factors like blade aerodynamic forces, blade reaction forces, material–mechanical properties, blade mass properties were determined and discussed. FEM analysis was done and stresses, strain, deflection of the blade were analyzed and discussed.

Wright et al. [17] measured the starting and low wind performance of a three-bladed, 2 m diameter horizontal axis wind turbine in field tests, and the results were compared with calculations done by employing a quasi-steady blade element analysis. It was observed that the blades started rotating at a wind speed of 4.6 m/s on average, but this varied between 2.5 and 7 m/s. The rotor acceleration values were predicted well, employing the composite lift and drag data of the airfoil and also generic equations at high angles of incidence. Various values of wind speeds for which the turbine rotor starts and ceases to rotate were determined. The accelerating, decelerating and the steady states of the rotor (in terms of blade angular velocity) were plotted for a range of rotor (0–500 rpm) and wind speeds (2–8 m/s) in Fig. 13. It can be observed that the starting wind speed was between 4 and 5 m/s.

A study and observations were made on the starting behavior of a small HAWT by Mayer et al. [18]. The calculations were done based on the classical blade element theory and wake modeling of a wind turbine of rotor diameter 5 m, producing 5 kW. The study shows that for a pitch angle of 0°, there was a longer idling period due to the very high angles of attack and the idling period decreased with the increase in blade pitch angle. It was also observed that at the pitch angle of 20°, shortest start was achieved. The angular velocity measurements for all the pitch angles were compared to those obtained by the integration of the angular acceleration equation. They also made use of the quasi-steady blade element analysis to determine the aerodynamic torque. The measured and the predicted angular velocity values agreed well with each other. The results did not match well at the lowest pitch (0°) due to the uncertainty in characterising the lift and drag at these high angles and extremely low Reynolds numbers.

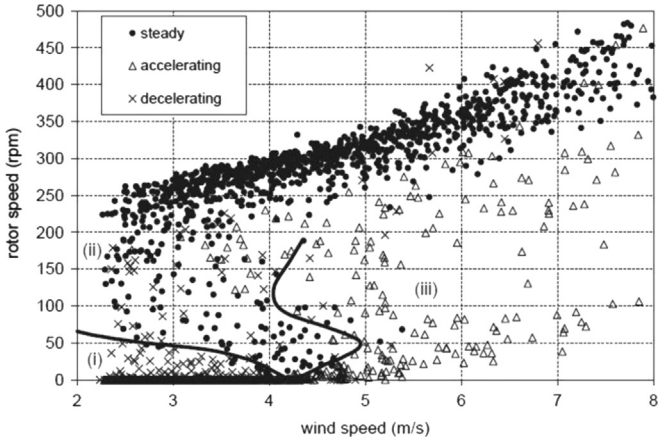

Fig. 13. Turbine low wind speed behavior [17].

Rocha et al. [19] have done a computational analysis on a small scale HAWT to calibrate a shear stress transport (SST) turbulence model regarding its operational capability. A 3-bladed wind turbine having NACA 0012 blade profile was designed for fixed tip speed ratio ($\lambda=5$). The experimental tests were carried out to evaluate the performance based on the power coefficient as a function of tip speed ratio. Power coefficient (Cp) plotted against the tip-speed using the experimental data, shows an average maximum C_p at $\lambda=7.25$ as shown in Fig. 14. It can also be seen that at the design TSR, there are no points of stalling. OPENFOAM, an open source CFD tool, was used to solve the shear stress transport turbulence model and assess the wind turbine performance. The experimental field data available for aerodynamic performance characteristic was required to calibrate the k-ω SST turbulence model. The turbulence intensity had no impact on the calibration of the model. For the same values of β^* (turbulence modeling constant), the results for I (free stream turbulence intensity)=2%, 20%, and 40% are almost the same and tends to coincide as the value of β^* increases.

Table 2 depicts the work done by various authors on HAWT in a single glance. From the work done by various authors, it can be observed that majority of the work has been concentrated on improving the performance of small scale HAWT by varying different parameters. A maximum power coefficient of 0.5 was observed when FX 63-137 was used and the average power coefficient was observed to be in the range of 0.2–0.35. Also, only Mayer et al. has worked on effect of performance of wind turbine when their fluctuation in wind velocity. This situation is very common for most of small scale wind turbines as these are placed at low heights (approx 10–15 m). These kinds of studies have to done in detail to know effect of actual wind conditions on performance of small scale wind turbines.

4.2. Blade design

Blade design is one of the most important parameters of interest in any type of wind turbine. This section presents the work done by various authors regarding the blade design. Lissaman [20] has performed a detailed study on low Reynolds number airfoils and has stated that a small degree of roughness needs to be

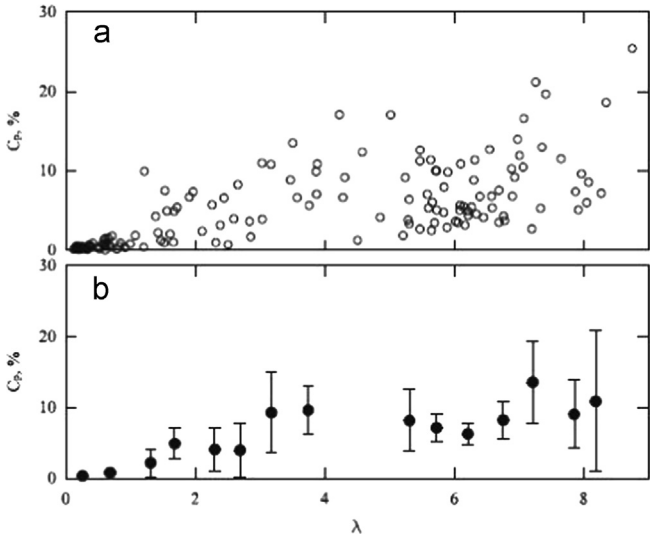

Fig. 14. Scatter plot of power coefficient C_p vs. tip-speed ratio 1 (a) as experimentally observed and (b) considering 95% confidence intervals [19].

Table 2
Summary of work on performance of small scale HAWT.

Authors	Airfoil	Rotor Diameter (m)	Wind speed (m/s)	Rotor speed (rpm)	Pitch angle	Max. C_P
Freere et al.	MG4520	2.1	Up to 13	50–600		0.2
Refan et al.	FX 63-137	2.2	1–11	0–1200		0.5
Singh et al.	AF300	1.26	7	500	15, 18, 20	0.255
Kishore et al.	–	0.394	<5			0.406
Hirahara et al.	NACA 2404	0.5	4–23	0–3000	18	0.4
Matsumiya et al.	SD7037	1.8	2.5–50	–	–	0.36
Chen and Liou	NACA 4415	0.9, 0.78, 0.59	6–12	–	–	0.45
Mayer et al.	–	5	–	–	0–35°	–

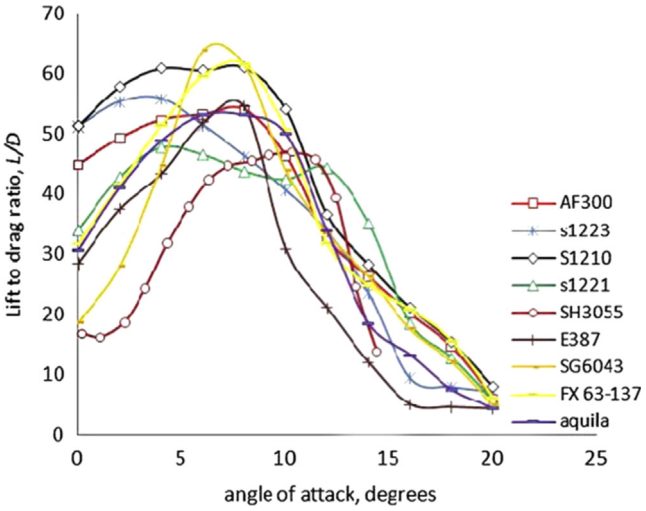

Fig. 15. L/D ratio, C_L values at different angles of attack plotted for 8 different blades [25].

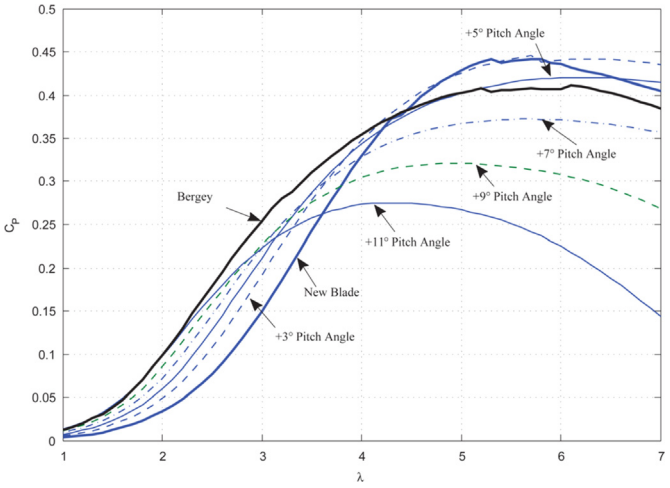

Fig. 16. BEM predictions of power coefficient for the new blades at different overall pitch angles, compared to the original Bergey blades [26].

associated with airfoils operating at low Reynolds number conditions. And also in order to promote the early transition from laminar to turbulent flow turbulators or trip wire devices could be introduced in order to eliminate laminar separation bubbles. Selig and Giguere [21] have studied the usage of specifically sized trip wires for high Reynolds number airfoils in order to induce early transition from laminar to turbulent flow. A new airfoil with high lift characteristics has been developed by Henriques and Silva [22] which works well in urban environment. This airfoil has C_L values close to 2 in the Reynolds number range of 6×10^4–1×10^6. Giguere and Selig [23] have experimented the applicability of SG series thin airfoils (SG6040–SG6043) for small scale wind turbine operations. These airfoils operate under a Reynolds number range from 1×10^5– 5×10^5. Selig and Giguere [21] also present the usage of 15 different airfoils mainly consisting of thin airfoils along the length of the blades. Selig and McGranahan [24] have conducted tests on six different airfoils which operate under a Reynolds number range of 1×10^5–5×10^5. Out the six tested airfoils, two airfoils namely FX63-137 and SH3055 were cusped airfoils. It was observed that these airfoils have an improved aerodynamic performance due to increased nose region and they have a C_L value of 1.8 in the desired zone.

In order to achieve better start up and low wind speed performance, an airfoil is designed for small HAWT applications. X foil was used for testing a number of existing low speed HAWT airfoils, in the design and optimization process. Singh et al. [25] performed experiments on the improved airfoil (AF300) in a wind tunnel at low Reynolds numbers. The AF300 airfoil was compared with 8 other airfoils designed for low Re application for small horizontal axis wind turbines. The L/D ratio, C_L values at different angles of attack were plotted for those 8 airfoils and compared with AF300 as shown in Fig. 15. For different angles of attack, the forces of lift and drag are calculated and pressure distributions over the surface of the airfoil are obtained. A CFD analysis was performed to get additional information on the flow characteristics. Particle Image Velocimetry (PIV) together with smoke flow visualization was used to study the flow around the airfoil. The maximum lift coefficients were obtained at the stall angle of 14°. The results from PIV and smoke flow visualization showed that the flow stayed fully attached to the airfoil surface from *Re* as low as 56,000 at an angle of attack 8° and maintained a fully attached flow up to 14° angle of attack for *Re* as low as 75,000.

Song et al. [26] have designed a small wind turbine blade using the blade element momentum (BEM) method for a three bladed, fixed pitch 1 kW HAWT. The blades were designed to fit Bergey XL 1.0 turbine, with 2.5 m diameter rotor, upwind orientation, rated power of 1000 W at 11 m/s wind speed and tip speed ratio of 5.85 and SD 7062 airfoil was selected. The test was done using a vehicle-based platform at the original designed pitch angle and also at 5° and 9° pitch angles. The new blades showed better aerodynamic performance in high speed wind conditions but under low wind speeds, the original blades showed better performance. The original blade was predicted to have higher Cp than the new blades at designed pitch (0°) and tip speed ratio λ less than 4.5, whereas at higher λ the new blades were predicted to have higher Cp values as shown in Fig. 16. The new blades at 5° pitch produced the highest power at wind speeds over 9 m/s, while the new blades at 9° pitch produced less power overall, but performed best at low wind speeds. The power output of the three blades was similar between 5 m/s and 9 m/s as shown in Fig. 17. Table 3 summarizes the work done by various authors on the blade design of a HAWT.

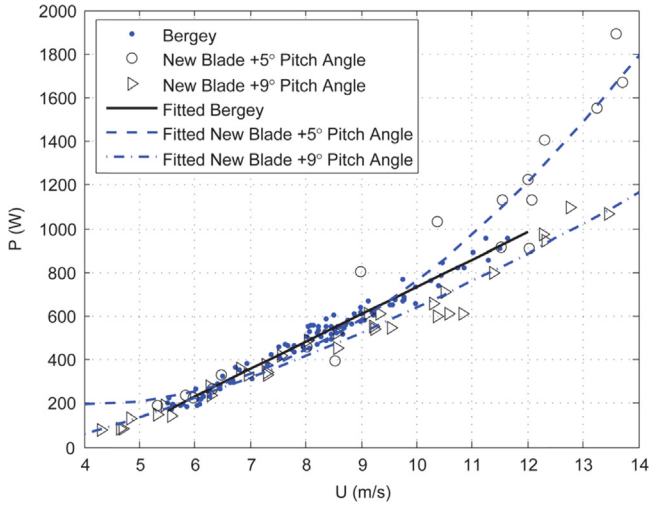

Fig. 17. Measured power curves for the new and original blades [26].

Table 3
Summary of work done by various authors on blade design.

Authors	Blade profile tested	Reynolds number
Giguere and Selig	SG6040–SG6043	1×10^5–5×10^5
Selig and McGranahan	S822, S834, E387, SD2030, FX63-137, SH3055	1×10^5–5×10^5
Singh et al.	AF300	–
Song et al.	SD 7062	–
Henriques and Silva	Designed a new airfoil	6×10^4–1×10^6

4.3. Control

Most of the small scale wind turbines control their direction using a tail vane. Due to high gyroscopic moment during sudden change of wind direction there is a possibility for the breakage of blades. A proper study on the control of yaw movement is necessary for small scale wind turbines.

An experimental study was carried out on passive yaw behavior of small scale HAWTs in order to examine the possible maximum yaw velocity, by Nishizawa et al. [27]. The model used was a 5 bladed, 1 m diameter turbine and uses 2 types of tail fins. Wind tunnel tests were conducted using a model wind turbine to investigate the yaw moment, restoring moment and yaw angular velocity corresponding to a change of yaw direction from 0° to 120°. The yaw behavior was studied for each tail fin, for a varied range of rotational speeds and wind speeds. It was observed that the rotor yaw moment is dependent on the tip speed ratio and at a yaw angle of 60°, the direction of the rotor yaw moment changed. For both tail fin types, the restoring moment was noted at the wind speeds of 6, 8 and 10 m/s and it was observed that the restoring moment increases with the increase of wind speed and the maximum value corresponds to a yaw angle of 120°.The yaw angular velocity increased with increase in the wind velocity and area of tail fin and decreased with increase in rotor rotational speed. It was observed that the maximum yaw angular speed was obtained at the wind speed of 10 m/s is 3.84 rad/s and it is greater than the conventional value of 3 rad/s.

A new theoretical equation of the yawing motion was derived by Watanabe et al. [28] in order to calculate the yaw rate (to estimate the yawing load), up to yaw angle of 180°, considering various design variables like rotor radius, design tip speed ratio, tail fin area and moment of inertia about the yaw axis. The calculations from this equation were compared to the wind tunnel test results and thus the equation was verified. A simplified equation to determine yaw rate for the small wind turbine with passive yaw system was derived and this new equation takes into account the sudden changes in the wind direction unlike the existing IEC standard as it considers all the design variables. Thus the yawing load can be estimated for large change of wind direction.

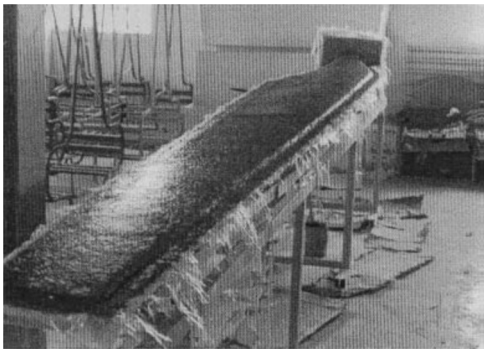

Fig. 18. Fiberglass and polyester resin laminates laid on the wooden model to get its shape [29].

4.4. Manufacturing of the blade

Habali et al. [16,29] manufactured and tested the blade and the blade rotor, which were designed by them. The rotor blade was designed as a combination of two airfoils FX66-S-196 and NACA 63-621. In the process of manufacturing the blade, first a wooden model was made to check parameters like continuity of the twist and smoothness of the surfaces. The Glass Fiber Reinforced Plastic mold was made and consisted of two parts: upper half and lower half which were strengthened using lateral rip stiffeners. The blade was then made in two shell halves in its respective molds and these shells were joined and glued together as shown in Fig. 18. The blade passed the Proof load test and later the performance testing of the rotor was done using electric measuring transducers. The cut in speed and the rated wind speed were found out to be 5 and 10 m/s, respectively. The rated power was found to be 16 kW and has exceeded the installed generator capacity (15 kW).

Mishnaevsky et al. [30] have studied the performance of small wind turbines with timber blades installed in several locations around Nepal. The different types of timber used for experiments were Lakuri, Pine, Sal, Saur, Sisau, Uttish, Tuni, and Okhar. They observed that pine and Lakuri due to their availability, inexpensiveness coupled with properties like high stiffness and breaking strain are the best viable option for wind blade material.

From the above section it was observed that many authors have mainly concentrated on effect of various parameters such as TSR, rotor speed, and pitch angle for a specific airfoil. Not much work has been done on the effect of airfoils on performance of small scale HAWT, effect of wind gust, and effect of turbulence intensity. Also, the airfoil design has to be optimized taking into consideration, ease of manufacturing and operation. Hence more work should be done on the above parameters in order to closely understand the characteristics of small scale HAWT.

5. Vertical axis wind turbine

Vertical axis wind turbine (VAWT) is a turbine in which the rotor axis is in the vertical direction. Since the rotor axis is in the vertical direction, these turbines need not be pointed into the wind to be effective make them advantageous for the usage on sites where the wind direction is highly variable. They are

significantly quieter than horizontal axis wind turbines making them particularly useful in residential and urban areas. But the VAWT's are less efficient that the HAWTs because of the additional drag they produce when the blades rotate into the wind. Hence efforts are being made to reduce the drag coefficient on the VAWT in order to make it more efficient. So the VAWT's are being tested on various parameters like wind velocity, tip speed ratio, solidity, rotor blade finish in recent years. Vertical axis wind turbines are mainly classified into two types:

- Darrieus type VAWT
- Savonius type VAWT

In addition to these there are other types of VAWT's such as the Sweeney type, Sistan type wind mill etc. which are not used frequently as the above two. This section presents the findings of various authors who have worked on these configurations of VAWT.

5.1. Darrieus type VAWT

First patented in the year 1931 by Georges Jean Marie Darrieus, a French aeronautical engineer, Darrieus type wind turbines are the most efficient of all the VAWT. All the Darrieus type wind turbines are lift based i.e. the rotor movement and the generation of electricity is caused by the lift forces acting upon the blades. The advantage of using this type of model is its simple construction and low cost. But there are certain problems associated with these turbines such as low starting torque, build integration, blade lift forces, and low efficiency. A 3 bladed Darrieus type wind turbine is shown in Fig. 19 below.

The work performed by various people on small VAWT is very less when compared to that of small scale HAWT. Much work on effect of various parameters on VAWT has not been studied as that of HAWT. Hence this review mainly focuses on the Numerical and Experimental studies done by various people on VAWT.

5.1.1. Experimental analysis

Takao et al. [32] have conducted experiments to study the effect of guide vane geometry on the performance of a Straight Bladed Vertical Axis Wind Turbine. The airfoil used for the study was NACA0018 having a chord of 100 mm, diameter of 600 mm and a height of 700 mm. The experiments were carried out in an open jet type wind tunnel having a diameter of 1.8 m. It was observed that the coefficient of performance was largely affected by the installment of guide vanes. It was noticed that the peak power coefficient was observed to be 0.205 which was approximately 1.8 times higher than the power coefficient of the wind turbine without guide vane. The reason behind this change is that the guide vane row changes the airflow inlet angle to the rotor radically.

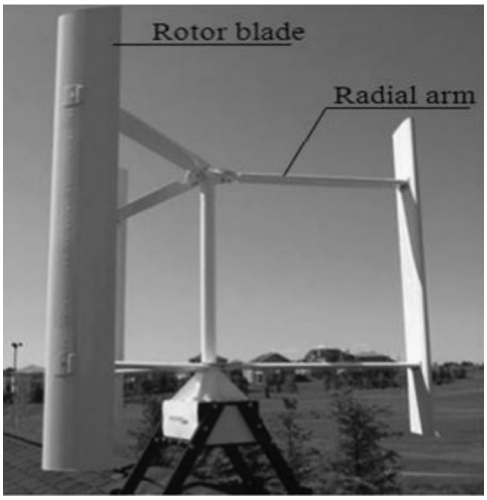

Fig. 19. Darrieus type wind turbine [31].

In the recent times, experiments have been performed by presetting the pitch of the blade. It was observed that by doing so, the coefficient of performance increases. Klimas [33] performed experiments on a 5 m diameter VAWT in Sandia National Laboratories on blade offset and preset pitch. Radius vector from the tower centreline to the blade chord at chord wise locations between 180% chord behind and 77% chord ahead of the leading edge with corresponding $\beta = -7^\circ$ to $+3^\circ$ were set and C_P was recorded. It was observed that at high tip speed ratio $\lambda = 5$, a C_P of 0.39 was recorded. McLaren et al. [34] investigated the effects of positive, negative preset pitch and blade mount point location offset on a 3-bladed high solidity, small scale, and H type-Darrieus VAWT with NACA 0015 blade profile with chord length of 0.4 m. It was observed that a blade with negative preset pitch improved the performance up to 29% while a positive preset pitch decreased the performance drastically up to 47%. It was also seen that the turbine recorded low power output as the blade mount point shifted towards the leading edge.

Apart from preset pitch, testing was also done on variable pitch mechanism. A brief description of the work is described below. Selig et al. [35] built a simplified blade pitch changing mechanism and tested in an open-jet wind tunnel. Effects of Reynolds number and tip speed ratio on the pitch configurations were studied. It was concluded that the performance of a fixed-pitch turbine could be enhanced by reducing the pitch angle and chord/radius ratio, or by using cambered blades. Turbines were found to perform better at higher λ as it reduces the angle of attack in the rear half and avoid stall. Miau et al. [36] focused on improving the starting torque of a small VAWT at low tip speed ratios using variable pitch. Both experimental and numerical analysis have been performed and it was found that the variable pitch records higher performance than the fixed pitch. Fixed pitch was performed for angles $\beta = -10^\circ$, 0°, and $+10^\circ$. The model was validated with the wind tunnel measurements of the static torque at 7 m/s with $\beta = 0^\circ$. It was found that in the variable pitch mode, $\beta = -70^\circ$ to $+70^\circ$ records high performance for λ of 0 to 2 against $\beta = -10^\circ$ to $+10^\circ$. Maximum $\alpha_{max} = 47^\circ$ was recorded to show significant improvements on aerodynamic torque for $\lambda = 1.1$ for $\beta = -18^\circ$ to $+18^\circ$.

Miley [31] conducted wind tunnel experiments on NACA 4 and 5 digit series prominently at low Reynolds number range. Selig et. al [35] also conducted tests in low speed, low turbulence, smoke tunnel at Princeton University on 54 different airfoils primarily designed for radio controlled model sailplanes. Further work by Selig and others resulted in a series of handbook on summary of low speed aero foil data from 2002–2010.

Table 4
Summary on experimental analysis of small scale Darrieus VAWT.

Author	Airfoil	Rotor diameter (m)	Pitch angle	Max. C_P
Takao et al.	NACA0018	0.6	–	0.205
Klimas et al.		5	-7° to $+7^\circ$	0.39
Mclaren et al.	NACA0015	2.5	$+/-3.9^\circ$, $+/-7.8^\circ$	0.34
Miau et al.	NACA0015	0.9	0°, -10°, 10°	0.55
Armstrong	NACA0013 NACA0015	2.5	$+2.5^\circ$, -1.5°, -3.5° and -5.5°	0.32

Armstrong et al. [37] investigated the aerodynamics of a high solidity vertical axis wind turbines through wind tunnel tests. An H type Darrieus wind turbine with a chord length of 400 mm was used with NACA 0015 as the blade profile. To understand the operating aerodynamics, flow visualization technique was used with light weight tufts attached to the inner surface of the blades. The aerodynamics was studied for canted blades along with straight blades. It was observed that the performance of the canted blades was different when compared to the straight blades. The possible explanation for this is due to the sweep of the blades and also the peak power and the blade tip speed ratio.

Table 4 summarizes the work performed on small scale Darrieus wind turbines. From the experimental analysis section, it was observed that work has mainly been done on NACA 0015 airfoil for different rotor diameters and pitch angles. It has been observed that a maximum power coefficient of 0.55 has been obtained for a rotor diameter of 0.9 m with effective pitch control.

5.1.2. Numerical analysis

In a review on various designs and configurations of vertical axis wind turbin.es by Bhutta et al. [38], it was concluded that CFD simulations predict the solution more accurately when compared to impulsive or Buckingham Pi theorem. Hence this numerical analysis section concentrates on the work by various researchers using CFD analysis.

Firstly we look at the numerical analysis work done on Straight Bladed Vertical Axis Wind Turbine (SBVAWT). Howell et al. [39] have studied the effect of two bladed and three bladed rotors on the performance of the straight bladed Darrieus VAWT's. The experiments were conducted on the NACA0022 airfoil with a thickness of 22 mm with a chord length of 100 mm and a height of 400 mm. They have observed that the performance of the wind turbine increases with the solidity. They have also observed that a small change in pitch angle causes dynamic stalling behavior and large and rapid changes in the force coefficients and rotor torque. At relatively low speeds, the performance depends upon the rotor surface finish and for a $Re > 30{,}000$, the performance can be increased by roughening the rotor surface.

Li et al. [40] investigated the feasibility and accuracy of three CFD approaches namely 2D URANS, 2.5D URANS and 2.5D Large Eddy Simulations(LES) in the aerodynamic characterization of Straight Bladed Vertical Axis Wind Turbines(SBVAWT) with a view to focus on the performance of the 2.5D scheme in high angle of attack flows. These approaches were examined by performing aerodynamic simulations on a single static NACA0018 airfoil having a chord of 200 mm for a 3 bladed SBVAWT rotating at different speeds. The obtained results were compared with the experimental results obtained in the wind tunnel tests by other researchers. The results showed that among the three approaches, 2.5D LES approach was in close agreement with both of the experimental results. It was observed that the 2.5D approach yielded more realistic 3D vortex diffusion after flow separation which helps in predicting the aerodynamic coefficients in dynamic and static stall conditions more accurately.

To obtain a mesh independent solution for a straight blade vertical axis wind turbine (SBVAWT) power curve using Computational Fluid Dynamics, four methods were numerically investigated by Almohammadi et al. [41]. These four methods include mesh refinement, General Richardson Extrapolation (GRE), Grid Convergence Index (GCI), and the fitting method. 2D Unsteady Navier–Stokes equations (URANS) with two turbulence models (Shear Stress Transport (SST) Transitional and Renormalized Groups (RNG) k-3 models) were employed to produce the solution. The results produced using the General Richardson Extrapolation method was found to be encouraging. But Grid Convergence Index showed an oscillatory behavior of the convergence which is not dependable. The fitting method can be chosen as a better alternative for the predicting the mesh independent power coefficient.

The effect of transitional turbulence model on a SBVAWT was discussed by Almohammadi et al. [42]. As flow around a SBVAWT is always complex, a proper turbulence model should be chosen for simulations. An investigation using S-A, RNG k-ε and SST k-ω models have been made in comparison to the SST transitional model for the laminar-turbulence transition assuming a fully developed flow. A sliding mesh technique was used solving 2D unsteady Reynolds averaged Navier–Stokes (URANS) equations. Significant changes were observed in the flow field and the stream lines and the trend of the normalized velocity magnitude profile is similar in the turbine upstream when the transition modeling is included. In the presence of the stall condition and/or the wake effect, turbulence model that accounts for the flow transition and the curvature correction to the turbulence production term is to be employed compulsorily.

Danao et al. [43] performed a two dimensional computational study in order to study the effects of rotor blade thickness and camber effects on a 5 kW VAWT. These results were validated by comparing them to the experimental results obtained for a pitching aero foil with dynamic stall phenomenon. The performance was carried out for different tip speed ratios to investigate why the performance of the turbine varies with varying blade thickness and camber. The blade profiles chosen for testing were NACA0012, NACA0022, NACA5522 and LS0421 as shown in Fig. 20. The results show that cambered profiles like LS0421 can improve the overall performance of the turbine but profiles like NACA5522 with a camber of 5% resulted in unfavorable performance. It was observed that the cambered profiles would cause the blades to produce high amount of torque both in upwind and downwind regions where as the inverted cambered profiles produce torque mostly in the upwind regions.

In order to evaluate the effect of aerodynamic and inertial contributions to the VAWT blade deformation, Castelli et al. [44] designed a computational model for a full RANS unsteady flow which was performed for NACA 0021 airfoil on a three bladed Darrieus turbine for a free stream wind velocity of 9 m/s. The torque coefficients were calculated as function of rotor azimuthal coordinate. This experiment was performed on various blade shell thicknesses and it was observed that the inertial contribution was higher than the aerodynamic contribution. The reason being, the inertial displacements were proportional to the blade thickness,

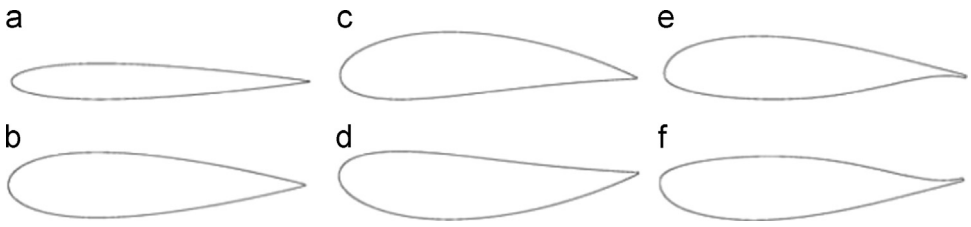

Fig. 20. Blade profiles used in the study (a) NACA0012 (b) NACA0022 (c) NACA5522 (d) NACA5522 inverted (e) LS0421 (f) LS0421 inverted [43].

which were connected to rotor blade mass. But the aerodynamic displacements were proportional to the rotor blade deformability which results in reduced blade thickness.

Several authors have performed experiments by varying different parameters on the performance of H-type Darrieus wind turbine. Mohamed [45] worked on the self-starting capability of the H-type Darrieus rotor and suggested some methods to improve this drawback. A numerical as well as experimental analysis has been performed to study the effect of solidity and the effect of using the hybrid system between the drag and lift types. The k-e turbulence model was used for qualitative and quantitative analysis of the performance of the turbine in unsteady state and also these steady simulations are used for calculating the static torque coefficients which is a measure of the self-starting capability of the turbine. The results indicate that the hybrid system improves the self-starting capacity of the turbine. But these experiments when performed for off design values showed that the hybrid system causes a significant decrease in the power coefficient suggesting that hybrid system is not a viable option for wind energy conversion. In case of solidity, it was observed that as the value of the solidity increases, the self-starting capacity also increases as shown in Fig. 21. And when checked for off design values, it was observed that a narrow operating range occurs at high solidity and also peak power coefficients occurs for low speeds by increasing the solidity.

McLaren et al. [34] have performed a Computational Fluid Dynamics simulation on a high solidity (σ=0.48) H-type Darrieus turbine and was solved for different blade speed ratios for a three blade rotor with constant flow velocity and the Reynolds number being 3,60,000. The high solidity, low blade speed ratio and rotational speed of the turbine gave rise to complex mechanisms which resulted in vortex shedding, vortex impingement and low momentum extraction. This resulted in reduced power production during the upstream pass while the reduction mainly occurs in the downstream pass which limits the thrust curves and generating the output. One small problem which occurred is that, since the flow is 2-D the turbine power and blade speed output have been over predicted. So, this can be corrected by incorporating a correction factor to the numerical inlet flow velocity which could effectively account for 3-D divergence.

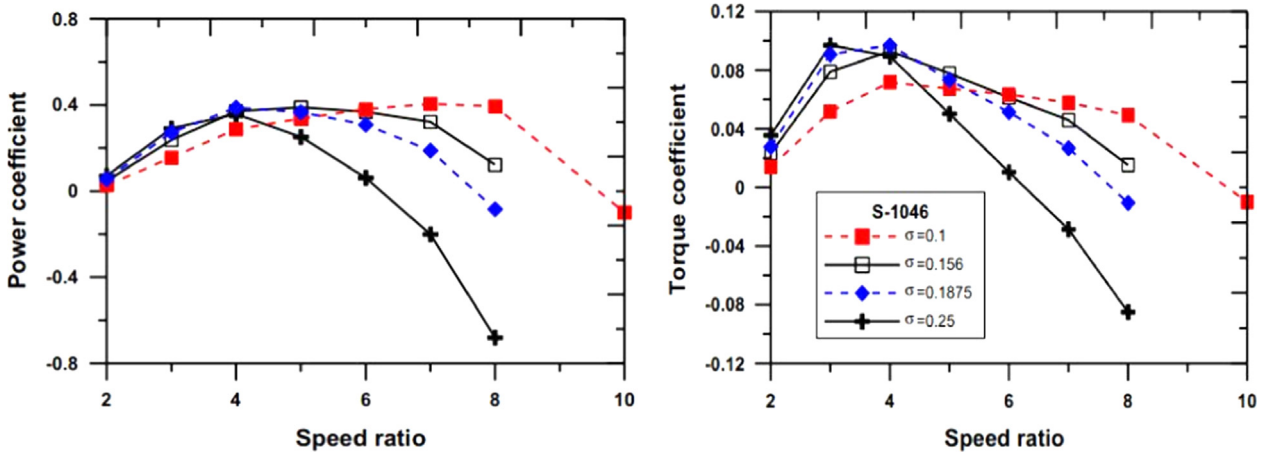

Fig. 21. Solidity effects on the performance of H rotor Darrieus turbine [45].

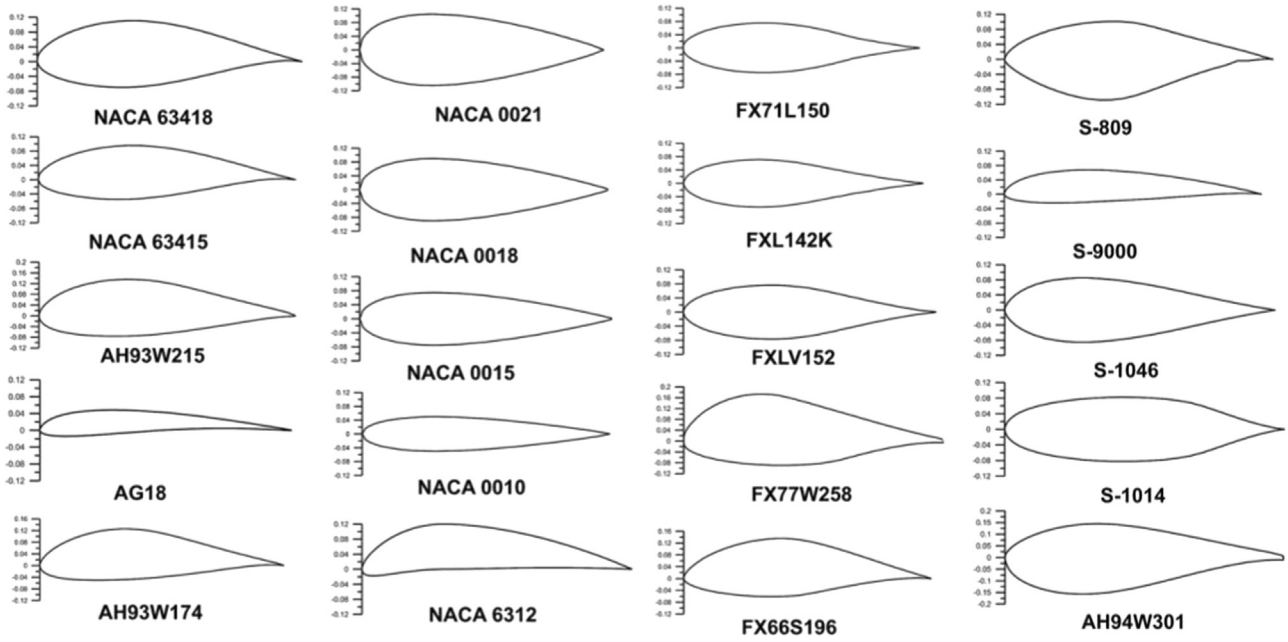

Fig. 22. Different symmetrical and nonsymmetrical airfoils used [46].

Mohammed [46] worked on increasing the torque coefficient and power coefficient for H-type Darrieus turbine by conducting experiments on 20 different air profiles as shown in Fig. 22. When these profiles were evaluated by using CFD, it was observed that there was an increase in the power coefficient of about 26.83% for the S-1046 when compared to the standard symmetric NACA airfoils which results in the increase of efficiency around 10.87%. And it was also suggested that low solidity is recommended for a wider operating range for the H-type Darrieus rotor in order to serve as a promising option for wind energy conversion.

Chowdhury et al. [47] have performed a comparative CFD analysis on VAWT in upright and tilted configurations in order to analyze the feasibility of operating VAWT on high rise buildings. Based on an existing experimental results, numerical analysis was performed and this was achieved by using CFD analysis. URANS model was selected and a brief parametric study was also done in order to choose the correct parameters. After simulating the turbine in both upright and tilted conditions it was observed that the numerical simulation data and experimental data were in good agreement. It is also understood that CFD simulation performs better than the BEM model in predicting the aerodynamic characteristics. Also, it was observed that the wake of tilted turbine moves downward since the wake of the tilted axis turbine moves downward in a tilted manner. This finding of the tilted axis turbines can be effectively used in sea surface utilization in offshore wind farms.

Elkhoury et al. [48] have performed experimental and numerical investigation on a micro-VAWT with a variable pitch. The turbine diameter and the blade span used were 800 mm respectively and the chord length used was 200 mm. The airfoil sections used were NACA 63_4-221, 0018 and 0021. The experiments for this following set up were performed in a wind tunnel whereas for the numerical simulations, in order to understand the flow structure, large eddy simulations with smagorinsky subgrid scale were used. The effects of various parameters such as wind speed, turbulence intensity, air foil shape, and strut mechanism with and without the pitch were studied and understood. It was observed that the numerical approach accurately predicted the performance of VAWT and also it was observed that thicker airfoils perform better with a considerable amount of pitch due to their better stall characteristics.

There are few studies on effect of unsteady wind on VAWT. Danao et al. [49] carried out experimental investigation on a wind tunnel scale vertical axis turbine with unsteady wind conditions. The radius and the height of the turbine are 0.35 m and 0.6 m respectively giving a solidity of 0.34. Wind speed of 7 m/s is tested with 7% and 12% fluctuation amplitude at 0.5 Hz frequency. Unsteady CP at 7% amplitude is almost same as the steady state. However at 12% fluctuation amplitude, there is drop in the mean CP value. The mean CP value for 7% and 12% fluctuation amplitudes are 0.26 and 0.18 respectively with mean steady CP of 0.205. Danao et al. [49] employed RANS based CFD modeling of VAWT to study the effects of steady and unsteady wind conditions. The turbine is three bladed with NACA 0022 air foil cross section. For the performance of the VAWT to be improved during unsteady state; the tip speed ratio is just above the tip speed ratio of the maximum steady CP, the fluctuation amplitude is less ($<10\%$), the fluctuation frequency is high (>1 Hz). Wekesa et al. [50] investigated the effect of airfoil of 12% and 22% thickness on the performance of VAWT in unsteady conditions using RANS based CFD modeling. Unsteady CP for NACA 0022 is 0.36 and that of NACA 0012 is 0.29. Hence in unsteady wind conditions, thicker air foils are desirable. For tip speed ratio greater than optimal tip speed ratio in steady conditions, thicker airfoils perform better compared to thinner air foils for the same tip speed ratio range. Wekesa et al. [51] investigated the performance of unsteady wind conditions on VAWT in Marsabit and Garissa, both towns in eastern regions of Kenya. Numerical analysis is employed using RANS based CFD modeling. Based on numerical analysis, the wind power and blade power at Marsabit are 698.43 W and 204.86 W while at Garissa are 33.59 W and -4.3 W respectively. Unsteady CP at Marsabit and Garissa are 0.3 and -0.13 respectively. The power density for Garissa and Marsabit are 47.99 W/m^2 and 997.76 W/m^2, a minimal drop of 17% and 4% from the empirical results respectively. The decrease in performance at Garissa station is due to the high wind speed fluctuations. Based on numerical analysis, Garissa station has wind class equivalent to 1, which makes it unsuitable for grid connected power generation. But Marsabit is found to have wind class equivalent to 7, making it suitable for grid connected power generation. Hence CFD is an alternate and inexpensive method to investigate the steady and unsteady analysis on the performance of VAWT.

Fig. 23. Savonius wind turbine.

Table 5
Summary on numerical analysis of small scale Darrieus VAWT.

Author	Model	Airfoil
Howell et al.	2D and 3D	NACA0022
Chao Li et al.	2D URANS, 2.5D URANS and 2.5D LES	NACA0018
Danao et al.	2D	NACA0012, NACA0022, NACA5522 and LS0421
Castelli et al.	3D	NACA 0021
McLaren et al.	2D	NACA 0015
Almohammadi et al.	2D URANS- SST and RNG k-3	NACA0015
Almohammadi et al. (Turbulence Model)	2D URANS- S-A, RNG k-ε, SST k-ω	NACA0015
Mohamed (2013)	2 D URANS and Realizable k-ε	NACA0021, S-1046
Mohamed (2012)	2 D URANS and Realizable k-ε	NACA0010, 0015, 0018, 0021, 6312, 63415, 63418; AG18, AH93W174, AH93W215, AH94W301, S-809, 9000, 1046, 1014; FX66S196, FX77W256, FX71L150, FXL142, FXLV152
Chowdhury et al.	3 D URANS and SST k-ω	NACA0018
Elkhoury et al.	3 D LES	NACA 63_4-221, NACA 0018, NACA 0021
Danao et al. [49]	2 D URANS and SST k-ω, Transition SST	NACA0022
Wekesa [50]	2 D URANS and Transition SST	NACA0012, NACA0022
Wekesa [51]	2 D RANS and SST k-ω	NACA0022

The trend in the normalized velocity magnitude profiles was observed to be different. Table 5 summarizes the various models and airfoils used by various authors in order to perform numerical analysis on small scale Darrieus wind turbines.

Table 5 summarizes the work done by various authors on the numerical analysis of small scale Darrieus wind turbines. From the above work, it is clearly understood that most of the work done by various authors are 2D simulations and a very few authors have worked on 2.5D and 3D simulation on Darrieus type wind turbines. Since 2D simulations do not match well with those of the experimental results, work focusing more on 3D simulations must be done in order to understand effectively the formation of vortices and angle of attack.

5.1.3. *Savonius type wind turbine*

The Savonius type wind turbine (as shown in Fig. 23) is a very important classification in the VAWT invented by the Finnish engineer Sigurd Johannes Savonius [52]. These turbines mainly operate on the principle of drag force.

A detailed review on the fluid dynamics aspects of Savonius wind turbine has been done by Kang et al. [53]. In this review flow patterns around Savonius wind rotors for conventional and spiral blade profiles with distributions of static pressures have been presented. Also optimal values of tip speed ratio which represent the maximum power/torque coefficient for various geometric shapes of Savonius wind rotors have been associated. Roy and Saha [54] have reviewed the numerical investigations on the design and development of Savonius wind rotors. A detailed study on various computational methods which demonstrate the influence of various parameters on the performance of Savonius wind turbines and their improvement techniques have been presented.

5.1.3.1. Experimental analysis. One of the major drawbacks of the Savonius turbines is the negative drag exerted on the convex part of the blades and the torque of the rotor varies in one rotation thus affecting the self-starting of rotor at different wind angles. Experiments were conducted by Emmanuel et al. [55] in order to improve the efficiency of Savonius turbines by increasing the number of blades and by preventing the wind from impinging on the convex parts. Results revealed that shielding the rotors can achieve a very high efficiency and having a six bladed rotor can achieve an efficiency of around 0.3.

Ali et al. [56] studied the performance of Savonius turbine to improve the efficiency by incorporating a flow restricting cowl. By testing different types of configurations as shown in Fig. 24, it was found out that the fully cowled configuration was the least efficient and it produced rotation only for high rotation speeds. However, the partially cowled configuration has produced a better efficiency for both centered and closed conditions. It was also observed that the closed position reduces the resistance and increases the rotational motion.

Experiments on Savonius rotor were conducted by Mohammed et al. [57] by attaching half-cylinder disks to the central rotor. Their work mainly focused on the concept of obstacle plate at the optimum configuration in order to increase the efficiency and utilize it mainly as an energy source for commercial purposes. Results showed that these considerations might make this type of turbine effective for domestic purposes.

An experiment was conducted by Plourde et al. [58] by installing VAWT on top of cellular towers and observed its performance

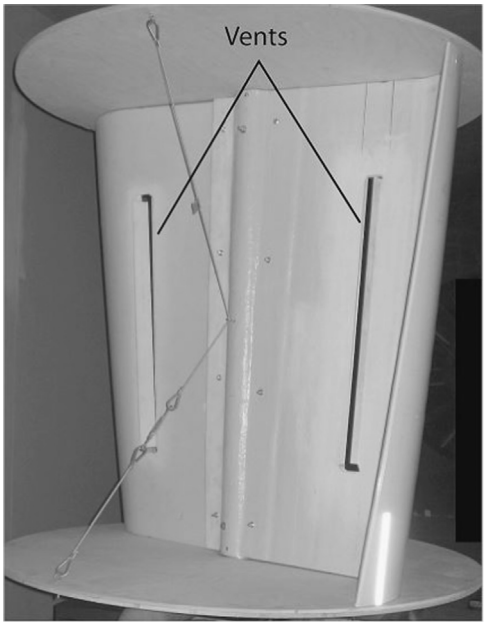

Fig. 25. Photograph of a capped and vented blade [58].

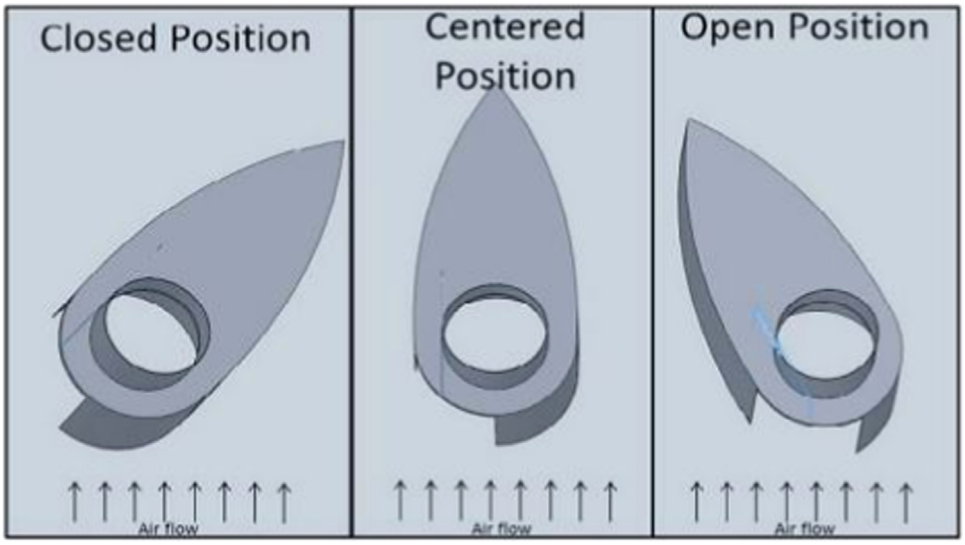

Fig. 24. Cowled configurations [56].

under various conditions air flow. It was observed that the capped turbines increase the power generation by a magnitude of 200 W for a speed range of 10 m/s and a magnitude of 270 W for a speed range of 11 m/s with electrical load being 78.7 Ω in both the cases for a single section. As there are four sections an additional power of 800–1100 W can be achieved. It was also concluded that the effect of venting on the performance of the VAWT is negligible as it does not affect the performance. A photographic view of capped and vented blade is shown in Fig. 25.

Damak et al. [36] have conducted experiments on a helical Savonius rotor with a twist of 180°. The aerodynamic study of the helical Savonius rotor was done and the effect of Reynolds number and overlap ratio on the performance of helical Savonius rotor was studied. These experiments were carried out in a cuboid shaped wind tunnel having a cross sectional area of 400 mm × 400 mm with the maximum air velocity being 12.7 m/s. It was observed that the rotor with the helical geometry yields better performance characteristics than that of the conventional one. It was seen that the helical Savonius rotor is very sensitive to the change in the Reynolds number.

In order to decrease the variation in static torque from 0° to 360°, experiments have been conducted on a helical Savonius rotor with a twist angle of 90° by Kamoji et al. [59]. The performance of helical Savonius rotor with and without end plates at different aspect ratios was studied and the obtained results were compared with the conventional Savonius rotor. It was observed that the helical Savonius rotor with shaft has the least coefficient of performance of 0.09 at a tip speed ratio of 0.9. When compared with the overlap ratios of 0.1 and 0.16, helical Savonius rotor at an overlap ratio of 0 has maximum coefficient of power of 0.174. The performance of the helical Savonius rotor was higher at lower aspect ratios as shown in Fig. 26.

Sheldahal et al. [61] have performed experiments on the effect of number of blades on the performance of Savonius wind turbines. Two, three and four bladed rotors have been used for testing. It was observed that two bladed rotors perform better when compared to three and four bladed rotors.

Zhao et al. [62] of a have performed experiments on a new type of helical bladed Savonius rotor and compared the results with that conventional Savonius rotor. It was observed that the optimum rotor power coefficient peaked at 0.2 for a two bladed rotor at a height to diameter ratio of 6.

Altan and Mehmet [36] have conducted experiments to study the effect of curtain design on the performance of Savonius rotors. The curtain was placed in front of the rotor in order to prevent the negative drag which is caused on the convex blade of the rotor. The performance of the rotor with and without the curtain was studied. It was seen that installing the curtain has a significant effect on the performance of the rotor. Out of the three curtains on which the experiments were performed, curtain 1 has given the best coefficient of performance at $\alpha=45°$ and $\beta=15°$ at its position $\theta=60°$. It was also observed that the coefficient of performance with curtain 1 is approximately twice than the rotor without any curtain. In order to verify the experimental results, a numerical model was developed and analysis was performed on the rotor having the curtain 1. It was seen that the numerical results and the experimental results closely match with each other.

Saha and Rajkumar [63] have conducted experiments on Savonius rotor with twisted blades and compared them with conventional semicircular blades. The performance analysis was done based on the factors like starting characteristics, starting torque and rotational speed. The twist angle was varied from 0° to 25° to understand how the performance coefficient varies accordingly. Experimental results showed that the rotor with the twisted blades showed better performance characteristics and self-starting capability than the conventional one. This happens because of the forces moving to the tip of the blade due to the induced twist on the blade. As a result a longer moment arm is generated giving a higher net positive torque. It was also observed that, with the increase in twist angles, the ability to capture energy on the lower arm reduces when compared to the upper part there by reducing the net positive torque.

5.1.4. Sistan type wind mill

Being one of the earliest turbines, the Sistan wind mill turbines (as seen in Fig. 27) were generally used in the areas of Sistan and Khorasan of modern Iran. These types of turbines are drag force driven turbines and can be constructed at ease. Having worked on the improvements in the traditional turbine design, Muller et al. [64] suggested that by adding disks at the top and bottom of the rotor, the efficiency of the turbine can be improved up to 30% and an additional increase of 6–7% in the efficiency can be achieved by increasing the number of blades from 4 to 6.

5.1.5. Twisted Sweeney type wind turbine

Sweeney who is well known for his “Princeton Sail wing Concept” wing for subsonic applications has proposed a vertical axis wind turbine driven by drag/lift force which was named after him as the Sweeney VAWT. But no tests were conducted by him on this turbine but some authors after testing this turbine in a wind tunnel have postulated the basic performance of the turbine. Later the Twisted Sweeney-type wind turbine was fabricated in order to increase the performance and enhance its external features. After a detailed study on this type of turbine Nemoto et al. [65] observed that by adding curvature to these turbines the power coefficient and the operational tip speed ratio increased significantly. By

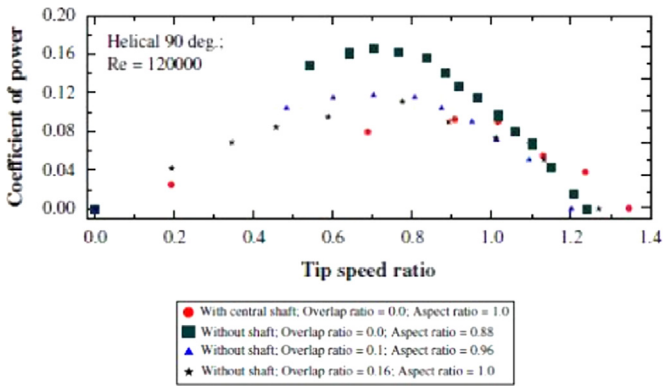

Fig. 26. Variation of C_p with TSR for 90° helical twist Savonius rotor [60].

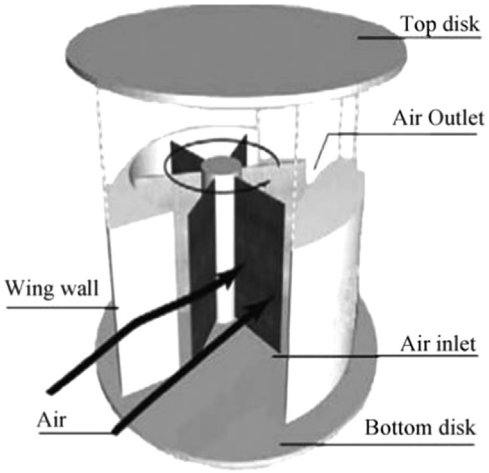

Fig. 27. Sistan wind mill [64].

Type	a	b	c	d	e
Cross section					
Shape					
Curvature	None	None	Small	Small	Large
Twist	None	Twisted	None	Twisted	Twisted

Fig. 28. Tested rotor configurations [65].

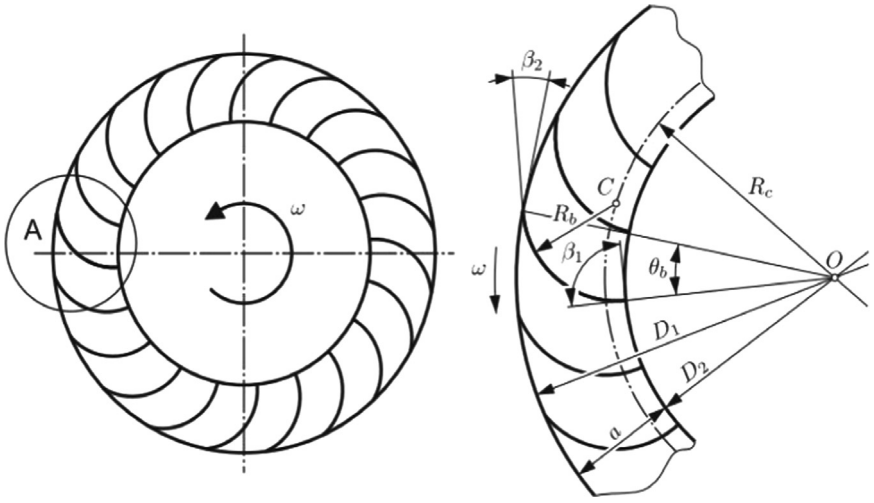

Fig. 29. Geometry of the cross flow runner [66].

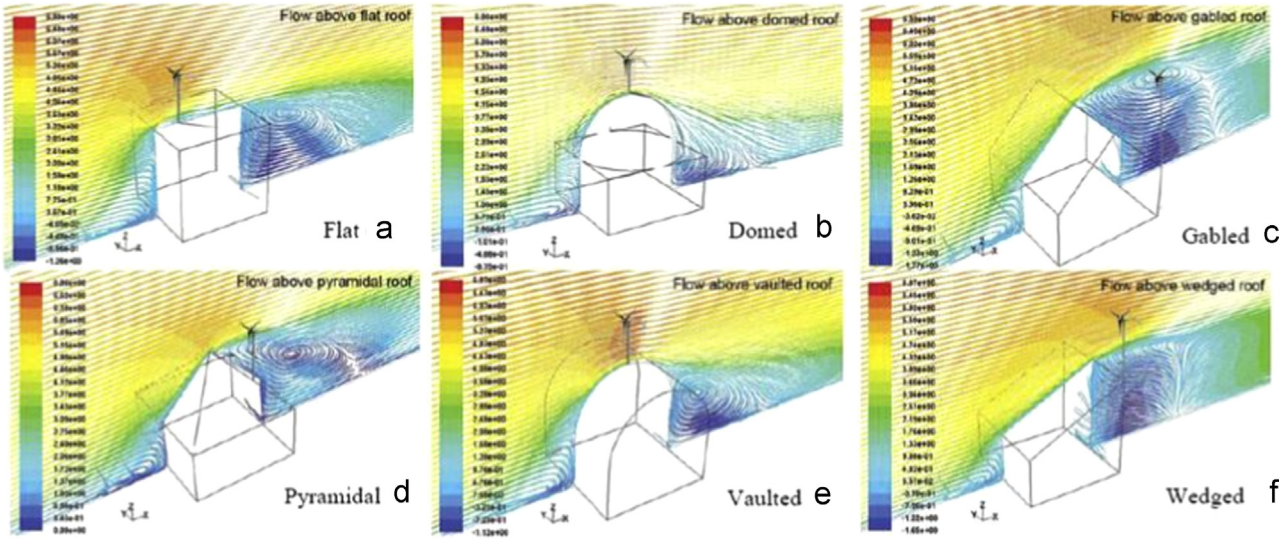

Fig. 30. Optimum mounting location for different roof shapes with 0° wind velocity direction [69].

twisting the blade as shown in Fig. 28, the power coefficient increased even at low speeds. And finally the power coefficient of the turbine with both twist and curvature is twice than that of an untwisted turbine.

One major problem with the VAWT is their inability to perform in low speed conditions. So, Dragomirescu [66] designed a VAWT with a cross flow runner (Fig. 29) to produce a better efficiency even in the low speed conditions. And it was observed that in low speed conditions the turbine can operate even at narrow tip speed ratios with the maximum being 0.6. A high starting torque coefficient of 3.6 has been achieved for such turbines which turned out to be greater than many other turbines. The turbine also produced a high power coefficient of 0.45.

6. Position of wind turbines

As mentioned earlier, small scale wind turbines can be used effectively used to fulfill domestic needs but the placement of these turbines also plays an important role in obtaining maximum efficiency. Various experiments have been conducted to determine the best suited position for the deployment of wind turbines.

According to Ledo et al. [67], the important factors which occlude the performance of the turbines are low mean wind speeds, high turbulence and high aerodynamic noise levels generated by the turbines. For example, if a turbine is subjected to high turbulence then there is a maximum possible chance for its blades to fail due to fatigue. Rafailidis [68] showed that the wind flow and turbulence levels at the roof top are mainly dependent on roof shape.

In an experiment conducted by Abohela et al. [69] to determine the optimum mounting position on top of the roof by considering various effects like roof shape, wind direction and building height as shown in Fig. 30. It was found out that maximum turbulence extends up to a height of 1.3H where H is the height of the building which indicates that the turbines should be positioned at a height equal to or greater than 1.3 times the height of the building.

Ayhan et al. [70] has reported wind aerodynamics and wind flows over the based on local meteorological data and local building characteristics. Also, technical review of various small scale wind turbines installed in building environment for power generation (as shown in Fig. 31). They concluded that in order to attain high wind power extraction and avoid turbulent areas, Computational Fluid Dynamics simulations have to be performed. They performed a simulation analysis for three different models of building integrated wind turbines. It was observed that the center of the roof rarely gives better efficiency than other mounting positions. And more over the difficulty in mounting the turbine at this position makes this position not a viable option for the deployment of wind turbine. As the shearing of wind is strong at the roof top, the mounting becomes difficult.

Grant et al. [71] performed experiments with ducted wind turbines and found it out as a viable alternative to the conventional machines which are attached to the roof buildings as they

Fig. 32. Pole mounted wind turbine [72].

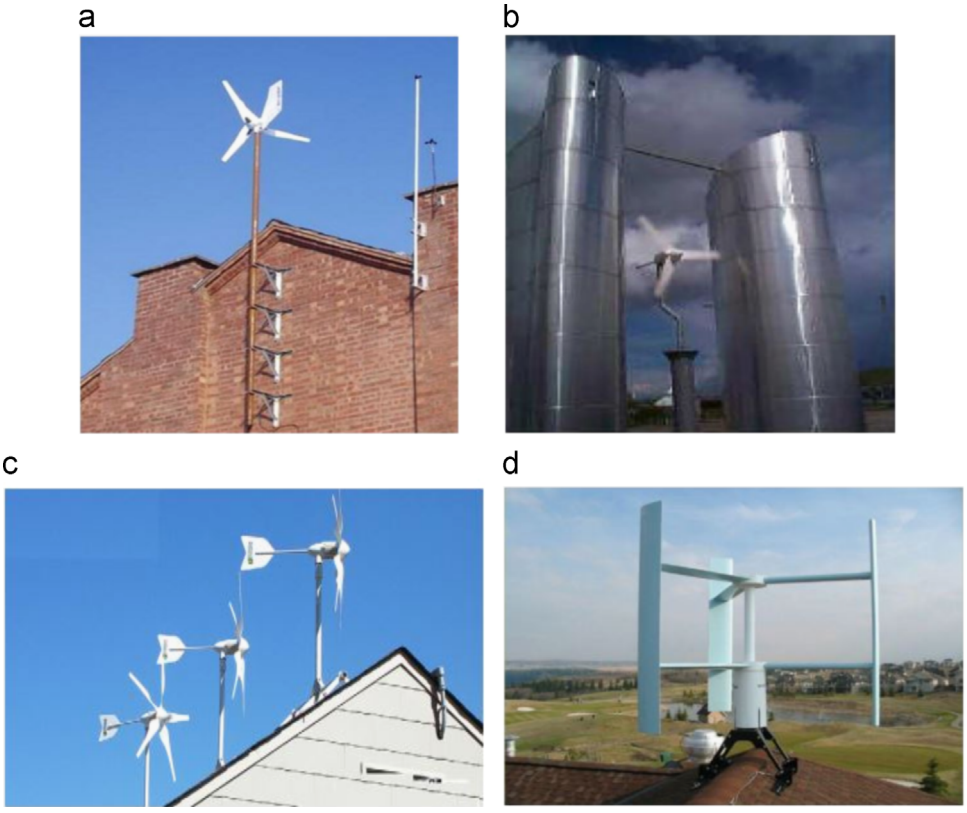

Fig. 31. (a)Wind turbine mounted on the gable end, (b) view of HAWT between buildings, (c) view of roof top HAWT and (d) view of roof top VAWT [70].

are protected from the turbulent effects and also as they have a very less visual impact.

Sissions et al. [72] performed experiments on pole mounted turbines as shown in Fig. 32 and found out that these can serve as a viable option to generate electricity and reduce carbon emissions when installed at sites with an appropriate wind resource. Results showed that, in order to achieve best efficiency, the minimum average wind speed should be at least 5 m/s at potential sites. Further research led to a finding which says that agricultural farms represent a highly attractive market for pole-mounted house hold wind turbine. So finally the optimum position for the deployment of wind turbines depends upon various factors like the roof shape, wind speed, turbulence intensity and surrounding conditions. Choosing the best position should be done carefully in order to achieve the best efficiency.

7. Aero acoustics

Aero acoustics is an important factor in designing wind turbine blades as it radiates acoustic noise. The dissonance that is created has to be considered in designing the wind turbine blade before installing it in a population dense region. The rotational speeds of most wind turbines develop constraints in designing of the blades because of acoustic emissions.

Migilore [73] presented the aero acoustic tests that were conducted on wind tunnels. These tests were to investigate the effect of boundary layer tripping, tip shape and trailing edge thickness on the acoustic emissions of a small wind turbine blade. These tests were done under realistic operating conditions with Reynolds number ranging from 170,000 to 397,000. Investigation was carried with six tip shapes, 3 boundary layer trip heights and 2 trailing edge thicknesses in a matrix of 72 velocity/angle attack test points. At low velocities (Reynolds number = 170,000), a difference of 3.8 dB was observed in overall sound pressure level between the extreme tip shapes and at greater velocities (Reynolds number = 315,000) a difference of 1.3 dB was observed. Based on the above results, a valid conclusion was made that tip shape is an important factor in reducing noise emissions from rotating wind turbine blades.

A method for reducing noises with a compromising power performance was presented by Clifton-Smith [74] called differential evolution technique. To predict power performance, differential evolution (DE) technique was coupled to an empirical noise prediction model with a blade element-momentum analysis. Starting time minimization was also done to improve low wind speed performance. The best trade-offs for 1% decrease in power coefficient were found to be a decrease in total sound pressure level (SPL) and starting time by 4% (2 dB) and 6% respectively, or a decrease in total sound pressure level and starting time by 1% (0.7 dB) and 16% respectively, at the TSR 5.5. The reduction to appropriate thin trailing edge noise using DE results in dominance of turbulent inflow noise out of the two most significant noise sources (turbulent inflow noise and turbulent boundary layer trailing edge noise). A trailing edge thickness of about 1 mm was found to be reasonable for reducing noise. Ghasemian and Nejat [75] studied the aero-acoustic prediction of a vertical axis wind turbine using large eddy simulation and acoustic analogy. Fowcs Williams and Hawkings acoustic analogy formulation was used to predict noises. Simulations were performed for five different tip speed ratios and the obtained mean torque coefficient was compared to that of the experimental data and a good agreement was observed. When researched for the broadband noises for turbulent boundary layers and tonal noises due to blade passing frequency, it was observed that there was a direct relationship between the strength of the radiated noise and the rotational speed.

Kim et al. [76] have designed an optimized airfoil of 10 kW class wind turbines consisting of three blades, a rotor diameter of 6.4 m, a rated rotating speed of 200 rpm and at a rated wind speed of 10 m/s. DU 91-W2-250 and DU 93-W-210 airfoils were optimized due to their good aerodynamic performance and maximum lift to drag ratio values. At design angle of attack, 7°, ratio of coefficient of lift to coefficient of drag (C_l/C_d) was 90, and improved by 51% in comparison with that of baseline of the new optimized airfoil which was 75% of blade position from root to tip. Numerical analysis of flow using X-FOIL and noise using WINFAS were done for incompressible flow and at Mach number 0.145 and Reynolds numbers 1.02×106. An overall reduction of 2.9 dB was found in SPL for the optimized airfoil.

In a survey done by Taylor et al. [77] the most commonly reported sounds of households close to micro- or small wind turbines have been presented. The survey showed that the most commonly perceived noises are ‘swooshing’, ‘humming’ and ‘whistling’, the presence of which may be inferred from the measured frequency spectra. In 5 kW wind turbines, low frequency sounds are dominant when compared to whistling. The above results were presented comparing the measurements taken at two installations with good results. The results show that people who are pessimistic about wind turbine installations receive more noises compared to others.

The results of investigation carried out to assess the effect of turbulence on the noise emissions from a micro-scale horizontal axis wind turbine (HAWT) were presented by Rogers et al. [78]. Two experiments were part of the investigation to find the noise emissions from a micro-wind turbine (MWT). The first experiment measured the one-third octave sound levels to quantify the sound spectrum for the MWT. In second experiment, the noise emissions from the same MWT due to the effects of turbulence were measured. Results found that doubling of the sound energy level was observed with doubling of turbulence intensity from 0.3 to 0.6. The reason for this increase in noise propagation was found to be because of delay in the rotor tracking the rapid changes in wind direction found at turbulent locations. Large aerodynamically produced sounds were observed when wind was not perpendicular to the rotor. Two distinct frequency ranges one between 120 Hz and 160 Hz at a sound pressure level barely audible to the human ear and the other between 2 kHz and 12.5 kHz typified broadband aerodynamic noises were observed. When a preliminary experiment was first examined with one-third octave noise spectrum for the micro-scale wind turbine with its peak value of 14 dB occurred at around 8 kHz.

Morris et al. [79] presented computational methods that can be applied to predict the aero acoustic noises. The concentration was mainly laid on low frequency noise generated by stall and trailing edge noise. The unsteady flow simulations were coupled to the radiated noise field with the permeable surface Fowcs Williams–Hawkings formulation. Linearized Euler equations were used for long range noise propagations predictions.

The issue of noise emission from a 2.3 MW SWT-2.3-93 wind turbine was addressed by Leloudas et al. [80]. Simulations were compared from a semi-empirical acoustic model with measurements. The comparison demonstrated a good agreement between predicted and measured noise levels as shown in Fig. 33. The acoustic model was further employed to carry out a parametrical study to optimize the performance/noise of the wind turbine by changing tip speed and pitch setting. Predicted noise contours were found to be function of pitch angle and rotational speed. The noise level increases as we move to higher rotational velocities (Fig. 34), however, the pitch angle also has an effect. At constant rotational speed, the noise increases as the pitch angle decreases (the angle of attack increases and the blade goes into stall).

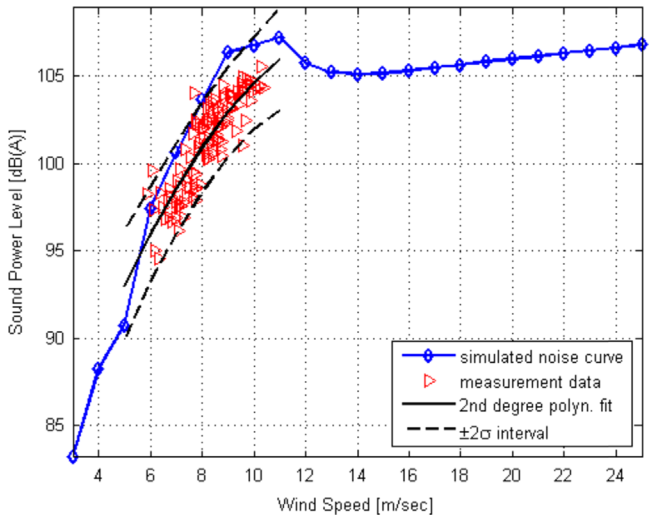

Fig. 33. Computed SPL vs. measurements for Siemens SWT-2.3-93 [80].

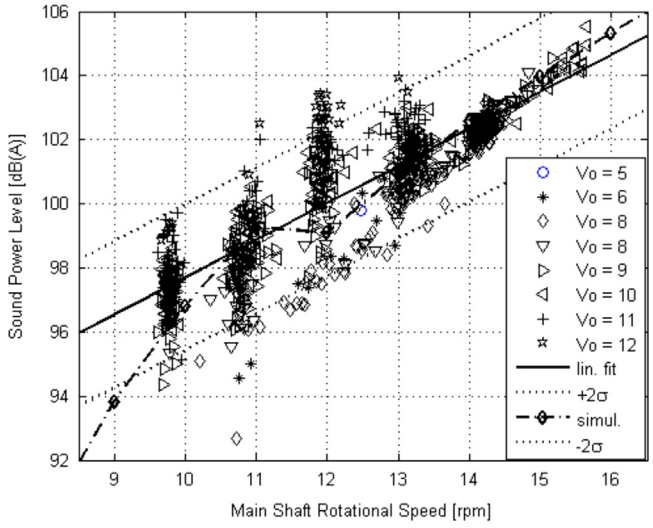

Fig. 34. Computed SPL vs. measured data as a function of rotational speeds [80].

Jianu et al. [81] reviewed recent advances in the area of noise pollution from wind turbines. His work primarily included analyzing and comparing different methods being implemented to reduce noises, with a focus on the noise generated from the trailing edge. He has also discussed about suppression of noises from mechanical sources such as generators, gearbox, hydraulic systems etc. using vibration suppression, vibration isolation and fault detection techniques. According to him, implementation of prevention strategies like adaptive approach and wind turbine blade modification methods can reduce the dominant source of noise (aerodynamic noise). Joo et al. [82] has performed numerical analysis with moving grid for various solidities and tip speed ratio's (TSR). 2 D and 3 D CFD analysis is done using Large Eddy Simulation (LES). Solidities 0.7 and 0.2 showed highest torque and angular velocities. But the largest efficiency occurred at solidity of 0.5, corresponding coefficient of power being 0.23. Authors attempted to explain the flow characteristics by two effects: Blockage and flow interaction between the blades and the free stream. For higher TSR's ($TSR > 3.7$) and solidity of 0.5, decline in torque is observed due to weak free stream in the downwind revolution because of blockage. When the TSR is low ($TSR < 2.2$) and solidity is 0.5, the angle of attack reaches the critical angle during upward revolution and the torque reduces. It is found that efficiency of 2 D analysis is more than 40%. However efficiency is 10–15% in case of 3 D analysis. Hence it is essential to conduct more studies on 3 D analysis of VAWT.

8. Findings from actual installation of small scale wind turbines

James et al. (2010) presented important findings of building mounted turbine component of the UK micro-wind trial undertaken by the Energy Saving Trust in 2008–09. Performance of 39 horizontal axis wind turbines in rural, sub-urban and urban areas is monitored. Majority of the micro-wind turbines do not receive sufficient wind resource to make them economical. Among the sites monitored, only two sites met with the NOABL-MCS standard of 5 m/s wind speed. In case of building mounted turbines, none of them reached the measured wind speed of 4 m/s. Regarding economics, micro-wind does not perform favorably compared to Photovoltaic under current policy and incentive regimes in UK. Due to the limited building mounted micro-wind turbines, there is favorable market of highly exposed rural sites. Sissons et al. (2011) discussed the key findings of pole mounted turbine (2.5–6 kW) component of the UK micro-wind trial and market assessment. They have overlaid the distribution of UK agricultural farms with the wind resource mapping to evaluate the number of potential agricultural farm sites for micro-wind. Assuming the acceptable payback period for the micro-wind turbine is set as 12 years at a discount of 12%, the minimum required load factor is 17% for 375 kW h/m^2 swept area. According to the estimation, there are 87,000 agricultural farms in UK that can provide a minimum load factor of 17% for pole mounted micro-wind turbine. At each site if 48 MW is installed at each site, a total of 4176 MW is generated. Considering market uptake level of 10%, would correspond to 418 MW of total capacity. The total annual generation that would be obtained is 1025 GWh. Grieser et al. (2015) empirically investigated the economic potential of small wind turbine (SWT) under different urban location settings and the important parameters for the investment decision making in Germany. Based on the turbine types, they found that HAWT's performed better in urban environment compared to VAWT. This is due to the relative advancement in HAWT that is obtained from large scale design. Authors stated that the feed in tariff proposed by Liersh could be a solution to foster SWT. SWT substantially improves the profitability of SWT due to higher grants offered and expands in outcome the areas in Germany where SWT can be operated profitably. Slight variation in wind speeds will cause significant effect on Net Present Value (NPV) and investment decision. Hub height of the installation and degree of urbanity are important parameters regarding economic feasibility. Kamp and Vanheule (2015) made a review on SWT sector in Kenya. They reviewed the status of the sector and the investigated the factors and dynamics that hinder sector growth. They employed Strategic Niche Management (SNM) and Multi-Level Perspective (MLP). The paper explains how the SNM and MLP approaches can be suited to review the renewable technologies in developing countries like SWT in Kenya context. MLP analysis revealed that socio-cultural factors and ingrained mindsets on the niche growth. They concluded that extensive study of social practices and cultural behavior is important while analyzing the external environment in case of developing countries. White and Wakes (2014) studied the effects of simple house shapes and heights (in New Zealand) on the characteristics of the air flow reaching the wind turbines employing Computational Fluid Dynamics (CFD). Since the government within New Zealand can put restrictions on the height of wind turbines, this paper calculated the optimized height of 15–20 m for potential electricity generation. Commercial CFD code Fluent is employed using K Epsilon turbulence model. This study is helpful for the government

to set a proper restriction on the wind turbine height and encourage the small turbine installers to make best usage of the wind resource by streaming resource permitting process for 15–20 m range turbine tower height.

9. Conclusions

As large scale wind turbines alter the global climatic conditions and have adverse effects on the atmosphere, small scale wind turbines offer a great scope for producing valuable power which can be sufficient for domestic needs without altering the climatic conditions. From the review, the following conclusions can be made:

1. For Small Scale HAWT, most of the work was focused on effect of various parameters such as TSR, rotor speed, and pitch angle for a specific airfoil. Not much work has been done on the effect of airfoils on performance of small scale HAWT, effect of wind gust, wind direction and effect of turbulence intensity. Also, the airfoil design has to be optimized taking into consideration, ease of manufacturing and operation.
2. As most of the small scale HAWT's are positioned over the buildings, it is expected to have reasonable wind velocity fluctuation and change in wind direction. Hence a detailed study on the effect of oscillation of wind velocity has to be performed in order to clearly understand the actual performance characteristics of small scale HAWT.
3. For small scale Darrieus VAWT, most of the numerical analysis has been performed in 2-D. Also, it was found that 2.5D and 3D yielded much better results when compared to 2D simulations. It is essential to perform 3D LES simulations to understand proper dynamics of VAWT. In the experimental part of Darrieus wind turbines, most of the experiments have been performed on a single airfoil. This work must be extended to other airfoils so that much better efficiencies could be obtained. Also, it was found that variable pitch would give higher Cp. But, it is essential to design low cost variable pitching mechanism which makes its viable for usage.
4. In order to achieve high power coefficient, the design should be positioned properly. Hence, it is necessary to study effective positioning of small scale wind turbines (especially horizontal) based on actual usage location to extract maximum power.
5. The dominant aerodynamic noises cannot be completely eliminated but can be minimized. This minimization can be done by improving blade shapes like trailing edge thickness, tail shape. A compromise on power performance should be done in order to achieve low aerodynamic noise radiations. The work done in this aspect is limited. It is essential to perform detailed experiments and simulations in this area to make small scale wind turbines viable to be used in populated areas.

References

[1] Bakshi I, Dhasmana I. Is power output a better guide for growth? Business Standard. New Delhi; 2015.
[2] Market Forecast for 2015–2019; 2014. Available from: ⟨http://www.gwec.net/global-figures/market-forecast-2012-2016/⟩.
[3] Global statistics; 2014. Available from: ⟨http://www.gwec.net/global-figures/graphs/⟩.
[4] Wang C, Prinn RG. Potential climatic impacts and reliability of very large-scale wind farms. Atmos Chem Phys 2010;10(4):2053–61.
[5] Fiedler BH, Bukovsky MS. The effect of a giant wind farm on precipitation in a regional climate model. Environ Res Lett 2011;6(4):045101.
[6] Kirk-Davidoff DB, Keith DW. On the climate impact of surface roughness anomalies. J Atmos Sci 2008;65:7.
[7] Keith DW, DeCarolis JF, Denkenberger DC, Lenschow DH, Malyshev SL, Pacala S, Rasch PJ. The influence of large-scale wind power on global climate. Proc Natl Acad Sci USA 2004;101(46):16115–20.
[8] Freere P, Sacher M, Derricott J, Hanson B. A low cost wind turbine and blade performance. Wind Eng 2010;34(3):289–302.
[9] Refan M, Hangan H. Aerodynamic performance of a small horizontal axis wind turbine. J Sol Energy Eng 2012;134(2) 021013–021013.
[10] Singh RK, Ahmed MR. Blade design and performance testing of a small wind turbine rotor for low wind speed applications. Renew Energy 2013;50:812–9.
[11] Kishore RA, Coudron T, Priya S. Small-scale wind energy portable turbine (SWEPT). J Wind Eng Ind Aerodyn 2013;116:21–31.
[12] Hirahara H, Hossain MZ, Kawahashi M, Nonomura Y. Testing basic performance of a very small wind turbine designed for multi-purposes. Renew Energy 2005;30(8):1279–97.
[13] Duquette MM, Visser KD. Numerical implications of solidity and blade number on rotor performance of horizontal-axis wind turbines. J Sol Energy Eng 2003;125(4):425–32.
[14] Matsumiya H, Ito R, Matsushita D, Iida M, Arakawa C, Kawakami M. Field operation and track tests of 1-kW small wind turbine under high wind conditions. J Sol Energy Eng 2010;132(1):011002.
[15] Chen TY, Liou LR. Blockage corrections in wind tunnel tests of small horizontal-axis wind turbines. Exp Therm Fluid Sc 2011;35(3):565–9.
[16] Habali SM, Saleh IA. Local design, testing and manufacturing of small mixed airfoil wind turbine blades of glass fiber reinforced plastics: part I: design of the blade and root. Energy Convers Manag 2000;41(3):249–80.
[17] Wright AK, Wood DH. The starting and low wind speed behaviour of a small horizontal axis wind turbine. J Wind Eng Ind Aerodyn 2004;92(14):1265–79.
[18] Mayer C, Bechly ME, Hampsey M, Wood DH. The starting behaviour of a small horizontal-axis wind turbine. Renew Energy 2001;22(1):411–7.
[19] Rocha PA, Rocha HH, Carneiro FO, Vieira da Silva ME, Bueno AV. k–ω SST (shear stress transport) turbulence model calibration: a case study on a small scale horizontal axis wind turbine. Energy 2013.
[20] Lissaman PBS. Low-Reynolds-number airfoils. Annu Rev Fluid Mech 1983;15(1):223–39.
[21] Giguere P, Selig MS. Low Reynolds number airfoils for small horizontal axis wind turbines. Wind Eng 1997;21(6):367–80.
[22] Henriques JCC, Marques da Silva F, Estanqueiro AI, Gato LMC. Design of a new urban wind turbine airfoil using a pressure-load inverse method. Renew Energy 2009;34(12):2728–34.
[23] Giguere P, Selig MS. New airfoils for small horizontal axis wind turbines. J Sol Energy Eng 1998;120(2):108–14.
[24] Selig MS, McGranahan BD. Wind tunnel aerodynamic tests of six airfoils for use on small wind turbines. J Sol Energy Eng 2004;126(4):986–1001.
[25] Singh RK, Ahmed MR, Zullah MA, Lee Y-H. Design of a low Reynolds number airfoil for small horizontal axis wind turbines. Renew Energy 2012;42:66–76.
[26] Song Qiyue, Lubitz William David. Design and testing of a new small wind turbine blade. J Sol Energy Eng 2014;136(3):034502.
[27] Nishizawa Y, Tokuyama H, Nakajo Y, Ushiyama I. Yaw behavior of horizontal-axis small wind turbines in an urban area. Wind Eng 2009;33(1):19–30.
[28] Watanabe F, Takahashi T, Tokuyama H, Nishizawa Y, Ushiyama I. Modelling passive yawing motion of horizontal axis small wind turbine: derivation of new simplified equation for maximum yaw rate. Wind Eng 2012;36(4):433–42.
[29] Habali SM, Saleh IA. Local design, testing and manufacturing of small mixed airfoil wind turbine blades of glass fiber reinforced plastics: part II: manufacturing of the blade and rotor. Energy Convers Manag 2000;41(3):281–98.
[30] Mishnaevsky Jr L, Freere P, Sinha R, Acharya P, Shrestha R, Manandhar P. Small wind turbines with timber blades for developing countries: materials choice, development, installation and experiences. Renew Energy 2011;36(8):2128–38.
[31] Miley SJ. A catalog of low Reynolds number airfoil data for wind turbine applications. NTIS; 1982.
[32] Takao M, Kuma H, Maeda T, Kamada Y, Oki M, Minoda A. A straight-bladed vertical axis wind turbine with a directed guide vane row—effect of guide vane geometry on the performance. J Therm Sci 2009;18(1):54–7.
[33] Maydew Randall C, Klimas PC. Aerodynamic performance of vertical and horizontal axis wind turbines. J Energy 1981:189–90.
[34] McLaren K, Tullis S, Ziada S. Measurement of high solidity vertical axis wind turbine aerodynamic loads under high vibration response conditions. J Fluids Struct 2012;32:12–26.
[35] Michael S. Selig, Donovan John Francis, Bruce Fraser David. Airfoils at low speeds; 1989. p. 62–63.
[36] Miau JJ, Liang SY, Yu RM, Hu CC, Leu TS, Cheng JC, Chen SJ. Design and test of a vertical-axis wind turbine with pitch control. Appl Mech Mater 2012;225:338–43.
[37] Armstrong S, Fiedler A, Tullis S. Flow separation on a high Reynolds number, high solidity vertical axis wind turbine with straight and canted blades and canted blades with fences. Renew Energy 2012;41:13–22.
[38] Aslam Bhutta MM, Hayat N, Farooq AU, Ali Z, Jamil SR, Hussain Z. Vertical axis wind turbine–a review of various configurations and design techniques. Renew Sustain Energy Rev 2012;16(4):1926–39.
[39] Howell R, Qin N, Edwards J, Durrani N. Wind tunnel and numerical study of a small vertical axis wind turbine. Renew Energy 2010;35(2):412–22.
[40] Li C, Zhu S, Xu Y-l, Xiao Y. 2.5 D large eddy simulation of vertical axis wind turbine in consideration of high angle of attack flow. Renew Energy 2013;51:317–30.
[41] Almohammadi KM, Ingham DB, Ma L, Pourkashan M. Computational fluid dynamics (CFD) mesh independency techniques for a straight blade vertical axis wind turbine. Energy 2013;58:483–93.

[42] Almohammadi KM, Ingham DB, Ma L, Pourkashanian M. Effect of transitional turbulence modeling on a straight blade vertical axis wind turbine. In: Germán Ferreira editor. Alternative energies. Springer; 2013. p. 93–112.
[43] Danao LA, Qin N, Howell R. A numerical study of blade thickness and camber effects on vertical axis wind turbines. Proc Inst Mech Eng Part A: J Power Energy 2012;226(7):867–81.
[44] Raciti Castelli M, Englaro A, Benini E. The Darrieus wind turbine: proposal for a new performance prediction model based on CFD. Energy 2011;36(8):4919–34.
[45] Mohamed MH. Impacts of solidity and hybrid system in small wind turbines performance. Energy 2013;57:495–504.
[46] Mohamed MH. Performance investigation of H-rotor Darrieus turbine with new airfoil shapes. Energy 2012;47(1):522–30.
[47] Chowdhury AM, Akimoto H, Hara Y. Comparative CFD analysis of vertical axis wind turbine in upright and tilted configuration. Renew Energy 2016;85:327–37.
[48] Elkhoury M, Kiwata T, Aoun E. Experimental and numerical investigation of a three-dimensional vertical-axis wind turbine with variable-pitch. J Wind Eng Ind Aerodyn 2015;139:111–23.
[49] Danao LA, Eboibi O, Howell R. An experimental investigation into the influence of unsteady wind on the performance of a vertical axis wind turbine. Appl Energy 2013;107:403–11.
[50] Wekesa DW, Wang C, Wei Y, Danao LAM. Influence of operating conditions on unsteady wind performance of vertical axis wind turbines operating within a fluctuating free-stream: a numerical study. J Wind Eng Ind Aerodyn 2014;135:76–89.
[51] Wekesa DW, Wang C, Wei Y, Kamau JN. A numerical analysis of unsteady inflow wind for site specific vertical axis wind turbine: a case study for. Renew Energy 2015;86(0):648–61.
[52] Ushiyama I, Nagai H. Optimum design configurations and performance of Savonius rotors. Wind Eng 1988;12(1):59–75.
[53] Kang C, Liu H, Yang X. Review of fluid dynamics aspects of Savonius-rotor-based vertical-axis wind rotors. Renew Sustain Energy Rev 2014;33:499–508.
[54] Roy S, Saha UK. Review on the numerical investigations into the design and development of Savonius wind rotors. Renew Sustain Energy Rev 2013;24:73–83.
[55] Emmanuel B, Jun W. Numerical study of a six-bladed savonius wind turbine. J Sol Energy Eng 2011;133(4):044503.
[56] Ali A, Golde S, Alam F, Moria H. Experimental and computational study of a micro vertical axis wind turbine. Procedia Eng 2012;49:254–62.
[57] Mohamed MH, Janiga G, Pap E, Thévenin D. Optimization of Savonius turbines using an obstacle shielding the returning blade. Renew Energy 2010;35(11):2618–26.
[58] Plourde BD, Abraham JP, Mowry GS, Minkowycz WJ. An experimental investigation of a large, vertical-axis wind turbine: effects of venting and capping. Wind Eng 2011;35(2):213–22.
[59] Erickson DW, Wallace JJ, Peraire Jaime . Performance characterization of cyclic blade pitch variation on a vertical axis wind turbine. In: Proceedings of the 49th AIAA aerospace sciences meeting including the new horizons forum and aerospace exposition; 2011.
[60] Kamoji MA, Kedare SB, Prabhu SV. Performance tests on helical Savonius rotors. Renew Energy 2009;34(3):521–9.
[61] Sheldahl RE, Feltz LV, Blackwell BF. Wind tunnel performance data for two- and three-bucket Savonius rotors. J Energy 1978;2(3):160–4.
[62] Zhao Zhenzhou. Research on the improvement of the performance of savonius rotor based on numerical study. Sustainable Power Generation and Supply. SUPERGEN'09; 2009.
[63] Saha UK, Rajkumar MJ. On the performance analysis of Savonius rotor with twisted blades. Renew Energy 2006;31(11):1776–88.
[64] Müller G, Jentsch MF, Stoddart E. Vertical axis resistance type wind turbines for use in buildings. Renew Energy 2009;34(5):1407–12.
[65] Nemoto Y, Anzai A, Ushiyama I. A study of the twisted sweeney-type wind turbine. Wind Eng 2003;27(4):317–21.
[66] Dragomirescu A. Performance assessment of a small wind turbine with cross-flow runner by numerical simulations. Renew Energy 2011;36(3):957–65.
[67] Ledo L, Kosasih PB, Cooper P. Roof mounting site analysis for micro-wind turbines. Renew Energy 2011;36(5):1379–91.
[68] N Meroney R, Leitl BM, Rafailidis S, Schatzmann M. Wind-tunnel and numerical modeling of flow and dispersion about several building shapes. J Wind Eng Ind Aerodyn 1999;81(1):333–45.
[69] Abohela I, Hamza N, Dudek S. Effect of roof shape, wind direction, building height and urban configuration on the energy yield and positioning of roof mounted wind turbines. Renew Energy 2013;50:1106–18.
[70] Ayhan D, Sağlam Ş. A technical review of building-mounted wind power systems and a sample simulation model. Renew Sustain Energy Rev 2012;16(1):1040–9.
[71] Grant A, Johnstone C, Kelly N. Urban wind energy conversion: the potential of ducted turbines. Renew Energy 2008;33(6):1157–63.
[72] James PAB, Sissons MF, Bradford J, Myers LE, Bahaj AS, Anwar A, Green S. Implications of the UK field trial of building mounted horizontal axis micro-wind turbines. Energy Policy 2010;38(10):6130–44.
[73] Migliore P, The potential for reducing blade-tip acoustic emissions for small wind turbines. Subcontractor Report SR-500-43472, NREL; 2009. p. 4.
[74] Clifton-Smith MJ. Aerodynamic noise reduction for small wind turbine rotors. Wind Eng 2010;34(4):403–20.
[75] Ghasemian M, Nejat A. Aero-acoustics prediction of a vertical axis wind turbine using large eddy simulation and acoustic analogy. Energy 2015.
[76] Kim T, Lee S, Kim H, Lee S. Design of low noise airfoil with high aerodynamic performance for use on small wind turbines. Sci China Ser E: Technol Sci 2010;53(1):75–9.
[77] Taylor J, Eastwick C, Lawrence C, Wilson R. Noise levels and noise perception from small and micro wind turbines. Renew Energy 2013;55:120–7.
[78] Rogers T, Omer S. The effect of turbulence on noise emissions from a micro-scale horizontal axis wind turbine. Renew Energy 2012;41:180–4.
[79] Morris Philip J, Long Lyle N, Brentner Kenneth S. An aeroacoustic analysis of wind turbines. AIAA Paper 1184; 2004.
[80] Leloudas Giorgos, et al. Prediction and reduction of noise from a 2.3 MW wind turbine. IOP Publishing. J Phys: Conf. Ser 2007;75(1).
[81] Jianu O, Rosen MA, Naterer G. Noise pollution prevention in wind turbines: status and recent advances. Sustainability 2012;4(6):1104–17.
[82] Joo S, Choi H, Lee J. Aerodynamic characteristics of two-bladed H-Darrieus at various solidities and rotating speeds. Energy 2015:1–13.